Understanding extracellular matrix stiffness dependent regulation of Golgi organisation and function in anchorage-independent breast cancer cells.

A Thesis submitted to

Indian Institute of Science Education and Research Pune in partial fulfilment of the requirements for the BS-MS Dual Degree Programme

by

Tushar Manik Sherkhane

Indian Institute of Science Education and Research Pune

Dr. Homi Bhabha Road, Pashan, Pune 411008, INDIA.

Under the guidance of

Dr. Nagaraj Balasubramanian

Associate Professor

From May 2023 to April 2024

INDIAN INSTITUTE OF SCIENCE EDUCATION AND RESEARCH PUNE

Certificate

This is to certify that this dissertation entitled '**Understanding extracellular matrix stiffness dependent regulation of Golgi organisation and function in anchorage-independent breast cancer cells'** towards the partial fulfilment of the BS-MS dual degree programme at the Indian Institute of Science Education and Research, Pune represents study/work carried out by **Tushar Manik Sherkhane** at Indian Institute of Science Education and Research under the supervision of **Dr. Nagaraj Balasubramanian**, Associate Professor, Department of Biology, during the academic year 2023-2024.

Tushar Sherkhane
BS-MS student
20191180
IISER Pune

Dr. Nagaraj Balasubramanian
Associate Professor
Department of Biology
IISER Pune

Committee:

Name of the Guide: Dr. Nagaraj Balasubramanian

Name of the TAC: Dr. Mayurika Lahiri

Declaration

I hereby declare that the matter embodied in the report entitled **'Understanding extracellular matrix stiffness dependent regulation of Golgi organisation and function in anchorage-independent breast cancer cells'** are the results of the work carried out by me at the Department of Biology, Indian Institute of Science Education and Research, Pune, under the supervision of **Dr. Nagaraj Balasubramanian** and the same has not been submitted elsewhere for any other degree. Wherever others contribute, every effort is made to indicate this clearly, with due reference to the literature and acknowledgement of collaborative research and discussions.

Tushar Sherkhane
BS-MS student
20191180
IISER Pune

Dr. Nagaraj Balasubramanian
Associate Professor
Department of Biology
IISER Pune

I would like to dedicate this thesis to all those who have contributed in my life in some way or other…!!

Abstract

Integrin-mediated cell-matrix adhesion is known to regulate cell growth and survival, which is deregulated in transformed cancer cells that acquire the ability to grow without adhesion, becoming anchorage-independent. Previous studies from the lab have established cell-matrix adhesion to be a vital regulator of Golgi organization and function. Studies have also shown that the Golgi organization is altered in cancer cells, which could affect cell-surface protein glycosylation, intracellular trafficking kinetics, and cargo sorting. Hence, here we have tried to understand importance of the extracellular matrix (ECM) stiffness has in regulating the Golgi organization and function and the role of differentially expressed genes has in regulating this, especially in the breast cancer cells because they are known for their stiffening and Mechanosensing.

Therefore, our study has tried to understand the role AXL could have in regulating the cell spreading and Golgi organization and function in the matrix stiffness dependent manner in breast cancer cells.

Acknowledgements

I would like to express my sincere gratitude to Dr. Nagaraj Balasubramanian for his guidance and support for the duration of my projects. I am very grateful for his inspiring guidance and support throughout the project. From the planning of the day to the planning the whole week and even month, executing this plan based on the possibilities, choosing what to pursue next and what to not, and making decisions smartly and logically is what I will always remember when it comes to him as a guide.

I would also like to express my heartful gratitude to my thesis advisory committee member, Dr. Mayurika Lahiri, Department of Biology, IISER Pune, for her guidance and valuable suggestions, for giving me expert guidance about my thesis during the mid-year evaluation as well as end-year MS thesis.

My special thanks to my PhD mentor, Arnav Saha, for his continuous guidance and mentorship in the lab throughout this project. Learning any experimental technique is one thing, and using that technique smartly, timely and in a planned way to answer defined questions is another thing. That's why I wanted to thank him for not just being an experimental guide but also being actively involved in the discussions, not only about the literature but also about the data that we get from the experiments.

Also, my warm regards and thanks to Antara Chakraborty, Debasmita Muzumdar, Shaunak, Mayuresh Konde, Prachi Joshi, Radhika Malaviya, Kajal Singh, Kajal Singh, Vaishnavi Raut and all past and present cell adhesion lab members for helping me out in learning the basic laboratory techniques during this period. I would also like to thank Dr. Angshuman Nag, Department of Chemistry, IISER Pune and his lab members for providing access to the lab instrument.

I would also like to thank Jayashree, Rutuparna, Aadishakti, Vaishnavi, Atharva, and Kajal, who have helped me train the mentor in me. It has been a great feeling to have someone to teach and someone to learn from at the same place, and these are people who have helped me re-learn all the things that I have learned from my seniors in the

lab. Also, thank you all for flooding me with simple looking questions regarding doing experiments, making presentations or any superficial but deep scientific discussions.

Therefore, I will always be thankful for being given this privileged opportunity and for providing an enriching experience by doing experiments, making scientific presentations/ posters, and even participating in weekly one-on-one discussions. These weekly one-on-one meetings, weekly lab meetings, and weekly journal clubs have entirely changed my perspective on the work of a particular lab and how it can contribute towards the growth of an individual. Working in the lab for the past two years has laid the foundation for my future research career. I am sure that the skill set and training I received in this research environment will tremendously help me accomplish my future aspirations.

I also want to express my deep gratitude to my family members and friends for their constant and timely support.

I thank Dr. Santosh, Mr. Vijay, and the IISER Pune microscopy facility. Also, I would like to thank the Department of Biology at the Indian Institute of Science Education and Research (IISER), Pune, for providing me with all the facilities and opportunities during this period. I would also like to thank INSPIRE for the fellowship during this five-year tenure at IISER Pune.

Finally, I extend my wholehearted warm regards to the IISER Pune for making me a part of this enchanting endeavour in this phase of life.

List of Figures

Table of Contents

Chapter 1: Introduction

Extracellular Matrix:

The extracellular matrix (ECM) is the extensive meshwork of the proteins and other biomolecules that surround, support, and give shape and size to the cells and tissues in the body. This helps in cell attachment and communications to the ECM and other cells and hence plays a vital role in cell functioning, like cell growth and movement. The composition of the ECM can vary in a cell/tissue-specific manner, and it forms a stable composite environment that contributes to its biomechanical properties (Yue, 2014). ECM contains different protein components, and collagen is the most abundant protein across various tissue types. Proteoglycans, elastin, and glycoproteins are also the other components of the ECM, each having distinct physical and biochemical properties which contribute to the overall properties of the ECM (Yue, 2014). This same ECM plays a role as a reservoir of various growth factors and bioactive molecules. That is why it plays a significant role in deciding the fundamental behaviour of cells like adhesion, proliferation, polarity and migration.

Cell adhesion:

If we consider any eukaryotic cell, it never exists as an individual entity. The other cells or cell types always make tissue work together to serve a larger purpose. Thus, it becomes more important for these cells to communicate with other cells or the surrounding them. Moreover, here comes the ‘cell adhesion’, which plays a vital role in cell-cell or/ and cell-matrix communication and regulation. This communication plays a crucial role in how the cell interacts or coordinates and determines cell behaviour in the complex environments inside the multicellular organisms (Khalili and Ahmad, 2015). Most mammalian cells are anchorage-dependent and will need this dependence for their regular survival and differentiation, migration and cell cycle. Therefore, cell adhesion is essential in stimulating the signals that regulate fundamental cell processes, as mentioned earlier (Huang and Ingber, 1999).

Cellular Mechanotransduction:

Mechanotransduction is the interpretation of the physical cues of the extracellular environment by the cells and their translation into the biochemical signalling pathways. In the complex micro-environments around the cells and inside the tissues, physical cues play as important a role as chemical cues in any living system. In such complex micro-environments, cells must examine the physical and mechanical properties surrounding the external environment and relay them inside by activating the signalling pathways. In a nutshell, this is cellular mechanosensing and cellular mechanotransduction.

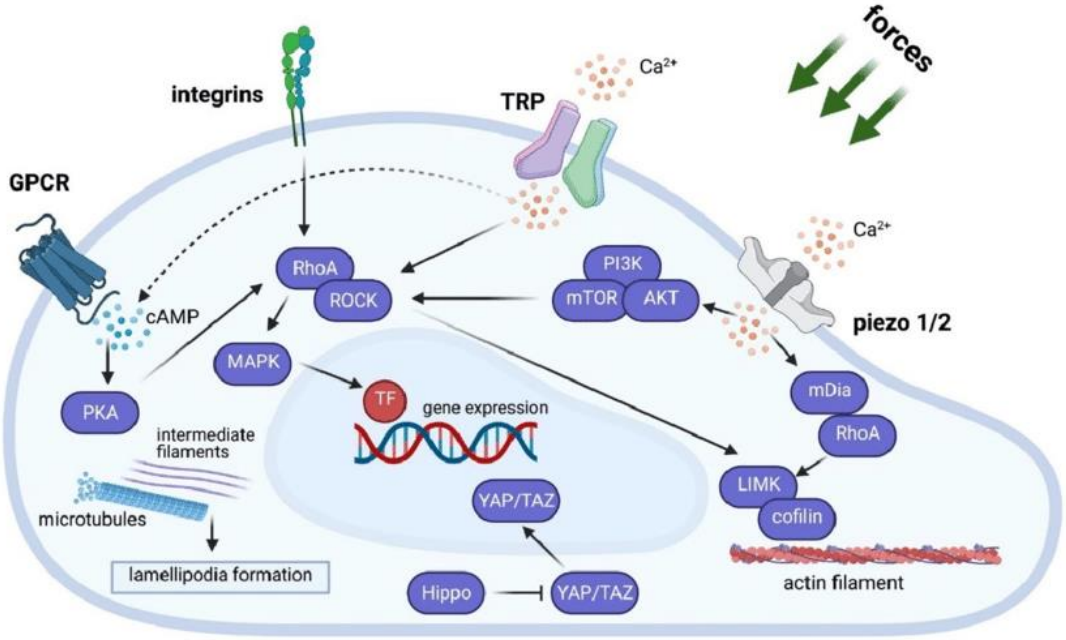

Figure 1.1: Generalized schematic for the Cellular Mechanotransduction (Elgindi et al., 2021)

There are various molecular mechano-sensors such as cell surface receptors, cell-cell junction receptors, cell-ECM focal adhesions, ion channels, and cadherins that cells use to sense the micro-environment around and transmit these mechanical cues to the intra-cellular with the help of biochemical signalling pathways in co-ordination with the intracellular cytoskeleton network (Jansen et al., 2017).

The sensation of the mechanical cues from the surrounding microenvironment and activation of the intracellular biochemical pathways represents the one-way directional

signal from the microenvironment to the inside of the cell. However, cells also produce signals that impact the microenvironment around them. This kind of bi-directional signalling between the cell-ECM or cell-cell is called mechano-reciprocity (Paszek and Weaver, 2004) (Van Helvert et al., 2018). It is also reported that intracellular organelles like the nucleus and mitochondria somehow respond to these mechanical cues (Feng and Kornmann, 2018).

Amongst the molecular sensors, integrins, a transmembrane receptor that binds to the specific ligands present in the ECM at the cell-matrix interface and hence acts as a link between the extracellular environment and the intracellular actin cytoskeleton network, are the most well-studied-and-widely-characterized (Jaalouk and Lammerding, 2009). The general theme of mechanotransduction pathways is that cells use mechanosensory receptors like integrins and cadherins to sense mechanical cues like shear forces, tensile strength and compression (Sun et al., 2016) (Liu et al., 2010). Also, proteins like talin, FAK, and vinculin are adaptors to connect these cell surface receptors to the intracellular actin filaments (Plotnikov et al., 2012). Then comes the various transcription factors like YAP and TAZ, which convey these mechanical cues to the inside of the nucleus, which leads to the change in the gene, protein, and metabolite expression profiles (Panciera et al., 2017).

Therefore, such protein and metabolite expression profile changes could directly affect cell spreading, proliferation differentiation and migration. The temporal scales of these mechanotransduction pathways can vary from milliseconds to seconds for sensing these cues. In contrast, hours are needed for the alterations in the gene expression and even days to affect the cellular behaviour (Iskratsch et al., 2014).

Adhesion and the regulation of the cell organelles:

As we discussed, the importance of integrin in cell adhesion and the importance of downstream signalling in growth factor signalling. This integrin-mediated adhesion regulates the various common downstream signalling pathways, such as MAPK signalling and PI3K-mediated AKT pathway (Kechagia et al., 2019). This integrin-mediated adhesion signalling and growth factor signalling is essential for many crucial cellular events like cell survival, proliferation, migration and gene regulation.

In the highly dynamic and crowded environment inside the cell cytoplasm, organelles experience various kinds of mechanical stresses. Specific organelles have evolved various mechano-signalling and transducing abilities to contribute towards the cell-ECM crosstalk. The nucleus and mitochondria are the primarily studied organelles and have well-established roles in cellular mechanotransduction (Barzilai et al., 2017).

The nucleus is also known as the stiffest organelle, which undergoes massive deformations by regulating the nucleoskeleton and is well-known and studied for its regulatory mechanosensory mechanisms (Dahl et al., 2004). A nucleus is an organelle that undergoes significant deformation while passing through the tight cell-cell junctions or dense meshwork of the extracellular matrix during extravasation and cancer cell metastasis. Another organelle known to be involved in the mechanotransduction pathways is Mitochondria. We know that mitochondria are responsible for cellular metabolism, and they are organelles that spread throughout the cytoplasm with the dynamic events of fission and fusion (Kraus et al., 2021). This structural integrity and the dynamics of fission-fusion events of the Mitochondria are regulated by the various physical forces and actin cytoskeleton network (Moore et al., 2016) (Carsten Johannes Helle et al., 2017). It has also been shown that integrin-mediated adhesion can regulate mitochondrial dynamics, and there are even studies which show that an increase in ECM stiffness regulates mitochondrial signalling via two different signalling pathways (Urra et al., 2021). Hence comes the question, can other cell organelles sense or respond to the extracellular matrix stiffness or the integrin-mediated signalling? Therefore, it is worth asking whether the dynamic organelle, like the Golgi apparatus, can respond to the physical parameters of the ECM or extracellular cues.

When it comes specifically to the Golgi, very little literature is available on the mechanosensitive characteristics of the Golgi apparatus. One of the studies from the lab has shown that cell-matrix adhesion can regulate the Golgi organization and function in normal anchorage-dependent cells. Upon loss of adhesion and integrin signalling, Golgi gets disorganized in the wild-type mouse embryonic fibroblasts (WTMEFs), which are well organized, ribbon-shaped, and have perinuclear localization in the stable adherent state. This regulation of Golgi is observed to be regulated via GTPase, named Arf1. Here, we have shown that active levels of Arf1 drop significantly upon the loss of adhesion. Moreover, we have also demonstrated

that this adhesion-dependent Golgi organization regulates its functions like trafficking and cell-surface glycosylation (Singh et al., 2018).

Other studies have also tried to reveal the novel mechanotransduction pathway operating at the Golgi apparatus. They have shown that reduction in the extracellular mechanical forces resonates with the way Golgi rheology is, which leads to the Lipin-1 inactivation and alterations of diacylglycerol levels at the Golgi apparatus. This also led to the reduced recruitment of Arf1 on the Golgi membranes (Romani et al., 2019).

Another study has shown that external mechanical stress applied to the Golgi affects membrane trafficking. They used confocal microscopy combined with the micromanipulation technique based on the optical trapping principle, and what they observed was a deformation of the Rab6+ membranes of the Golgi and also the disruption of the Golgi-associated actin (Guet et al., 2014).

Such studies lead us to explore newer and novel ways to study and understand the mechanical aspects of organelle functioning, especially its regulation of organelles like the Golgi. Furthermore, such a body of work encourages us to ask if and how such a regulation could be affected in diseases like cancers, known to have altered Mechanosensing capabilities. Hence, we have evaluated the differential regulation of Golgi organization across different cancers. We have also assessed the role and regulation of the Golgi in response to changing matrix stiffnesses.

Anchorage Independence and Cancers:

When it was first proved that cancer cells have anchorage-independent properties, cellular mechanotransduction became particularly important in understanding cancer cell regulation and function. Normal cells and tissues must attach to the substratum for normal signalling and survival. Hence, there is a finely tuned homeostatic balance between cell-ECM attachment. As mentioned, this integrin-growth factor crosstalk gets deregulated in the malignant transformed cells by activating oncogenes and losing tumour suppressor genes. Therefore, the transformed cancer cells do not require anchorage for survival, so they are called anchorage-independent cells. This anchorage-independent growth of the cancer cells is a direct readout of the

constitutive active anchorage-independent signalling pathways (Guadamillas et al., 2011).

Breast cancers and their mechanobiology:

One of the hallmarks of breast tumours is tissue hardening, which is thought to contribute towards the malignancy of normal breast epithelial cells. Mechanical stress and cellular responses are present in normal physiological conditions. Still, there is a variety of breast cancer-associated physical cues present in the breast tumour microenvironment, which are pathophysiological. Mechanical stressors like an increase in stiffness, solid stress or an increase in the interstitial fluid pressure are physical parameters in the tumour microenvironment responsible for the tumour progression (Xu et al., 2023). The average breast tissue is known to have stiffness within the range of 0.5 kPa to 2.5 kPa, whereas the breast cancer tissue is over 4 kPa and can go even beyond 20 kPa (Liu et al., 2021). In opposition to the increased breast cancer tissue stiffness, adjacent tissue stiffness is also affected. Animal model studies have also suggested that when breast tissue becomes more invasive, the adjacent matrix tissue gets stiffer than distant normal tissues. This happens because of the abnormal changes in the composition and structure of the tumour extracellular matrix in the breast cancer tissue (Xu et al., 2023).

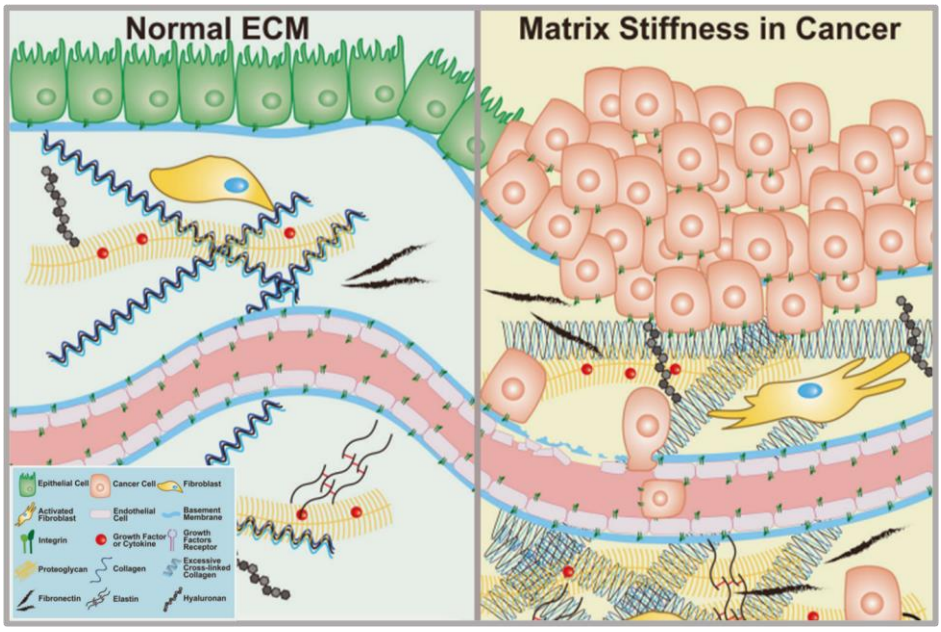

***Figure 1.2**: Normal tissue vs. stiff tissue in Cancers (Modified from Tian et al., 2022)*

Golgi organization and cancers:

The Golgi apparatus is known to be dramatically affected in various cancers by its structure and function. The substantial work has also shown that Golgi organization in specific cancer types is known to be disorganized or dispersed (Petrosyan, 2015). In contrast, some cancer cells are known to maintain the cisternal organization of the Golgi but lack the typical ribbon organization like normal mammalian cells. Also, Golgi is not only found to be completely disassembled or fragmented in specific cancer types but also has normal organization, as observed in anchorage-independent mammalian cells. These changes or defects in the Golgi morphology across various cancers can be linked to oncogenes and tumour suppressor gene mutations. Do these altered Golgi phenotypes have any role to play in the tumorigenic properties of the cancer cells, or is it just the consequence of the epithelial-to-mesenchymal transformation process? Because it is known that Golgi undergoes dramatic morphological changes during the epithelial-to-mesenchymal transition (EMT) (Tan et al., 2021).

Recent studies have deepened the role and regulation of the Golgi in cancers. One of the studies has shown that loss of p53 leads to upregulation of PAQR11 expression and promotes secretion of pro-metastatic soluble factors in the tumour microenvironment via the Arf1 recruitment of the Golgi membranes (Tan et al., 2021). Cancer cells are known to undergo anoikis resistance, and the probable mechanism by which they acquire anoikis resistance is by regulating the expression levels of the integrin on the cell surface. Downregulation of the GRASP55 levels disrupts Golgi organization, which reduces the expression of α5β1 integrin (Ahat et al., 2019).

Also, a functional readout of the altered Golgi morphology across various cancers can be seen as an altered protein glycosylation, which aids in the established hallmarks of the cancers. Depletion of the Golgi matrix proteins like GRASPs has been reported to increase protein trafficking through the Golgi, which is accompanied by decreased levels of glycan complexity and levels with inaccurate protein sorting because it disrupts Golgi (Xiang et al., 2013).

Golgi phenotypes screening across various cancers:

In the lab, Golgi organization phenotypes were looked at using a simple screen across multiple cancers, including lung, bladder, and breast cancer, to check the organization of the Golgi apparatus in these cancer cell lines. This work was done by a graduate student in the lab, Prachi Joshi.

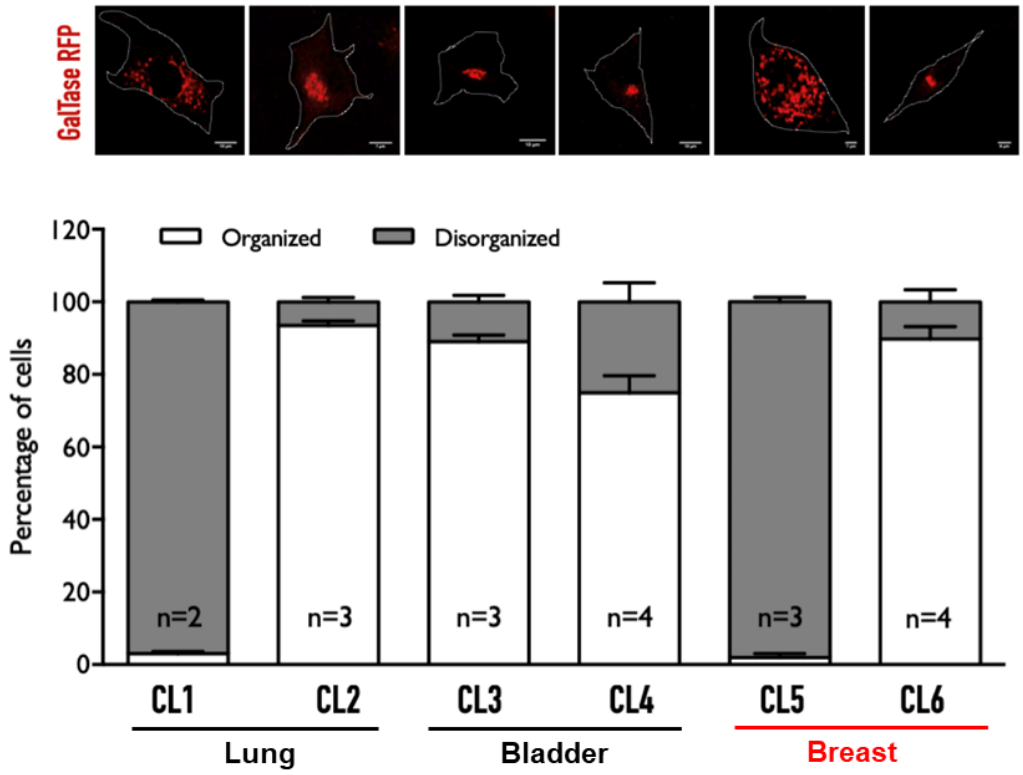

Figure 1.3: *Golgi organization screening across various cancers. (unpublished data - Prachi Joshi)*

Breast cancer cell lines and differential Golgi organization:

Among all the cancers screened for the Golgi organization phenotypes, we chose the breast cancer cell lines (MDMAB231 and MCF7) to proceed with because of their differential cell-specific characteristics. Despite both being breast carcinoma cells, they showed distinctly different Golgi phenotypes. MDAMB231 cells have a predominantly organized Golgi organization, whereas MCF7 has a predominantly disorganized Golgi phenotype.

As discussed earlier, adhesion can regulate the Golgi organization, More precisely, upon loss of cell-matrix adhesion, it is observed that Golgi undergoes dramatic disorganization. Both of the breast cancer cell lines that we have chosen to study are anchorage-independent cell lines. They have also shown contrasting Golgi phenotypes in the stable adherent state. Hence, we wanted to ask whether cell-matrix adhesion affects the Golgi organization of these cell lines. When these cells were detached and held in the suspension, MDAMB231 cells, which predominantly have organized Golgi phenotype in a stable adherent state, became predominantly disorganized. But, for MCF7 cells, when held in the suspension, Golgi remains disorganized (Fig 3.1 A). This suggests that though cell lines are anchorage-independent, the regulation of the Golgi organization in these two is differentially regulated. The regulation of Gogi in MDAMB231 cells is anchorage-dependent, but in MCF7 cells, it is anchorage-independent.

In-silico analysis to identify the regulators of differential Golgi organization:

Differential expression of genes could contribute to the differential regulation of Golgi organization in these two breast cancer cell lines, i.e. MDAMB231 and MCF7. A detailed in-silico analysis of databases (which ones were used) accompanied by data from literature and network analysis of genes helped shortlist genes that could be differential expressed (DEGs), have Golgi localization, and thus possibly regulate Golgi organization or function between these two cell lines. This multi-step in-silico approach has identified 20 DEGs as possible candidates that could regulate differential Golgi organization between these two. Amongst these, 11 genes were found to be upregulated in MDAMB231 compared to MCF7, which led us to test the role of these genes in regulating the differential Golgi organization and Mechanosensing.

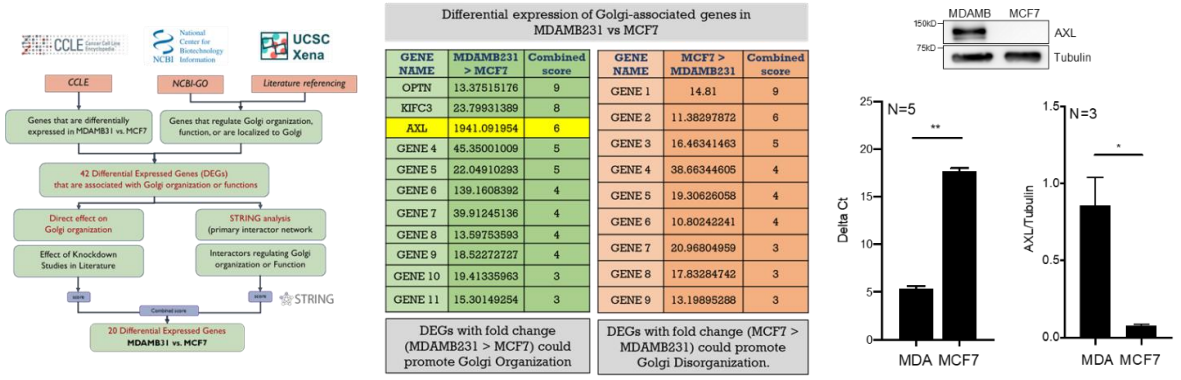

Figure 1.4: *Steps for the in-silico analysis for DEGs and the list of DEGs. Verification of the AXL expression levels using RT-qPCR and Western blotting. (Unpublished data – Arnav Saha, Debiprasad Panda, Grishma Mehta)*

As a first, we chose the AXL gene, one of the top 3 candidates in the in-silico screen, because of its complete absence in the MCF7 and its significant upregulation in MDAMB231 cells. Then, we confirmed the AXL protein and mRNA expression levels in these two cells using western blotting and RT-PCR, and they both demonstrated significantly higher AXL levels in MDAMB231 relative to MCF7.

AXL: A receptor tyrosine kinase

AXL is the cell-surface receptor tyrosine kinase and belongs to the TAM (TYRO3, Axl, and MER) family of RTKs. This tyrosine kinase receptor AXL is known to be an oncogene that increases cancer cell proliferation, survival, migration, and invasion, promoting cancer development. It has also been shown to be in cancer cell resistance to chemotherapeutic agents. It is also found to be upregulated in triple-negative breast cancers and is a promising therapeutic target. Though the tyrosine kinase activity is strictly regulated in the normal cells, they tend to gain the transforming function because of the mutations, over-expressions, and autocrine or paracrine stimulation, which results in the form of malignancy of the tissues (Paul and Mukhopadhyay, 2012).

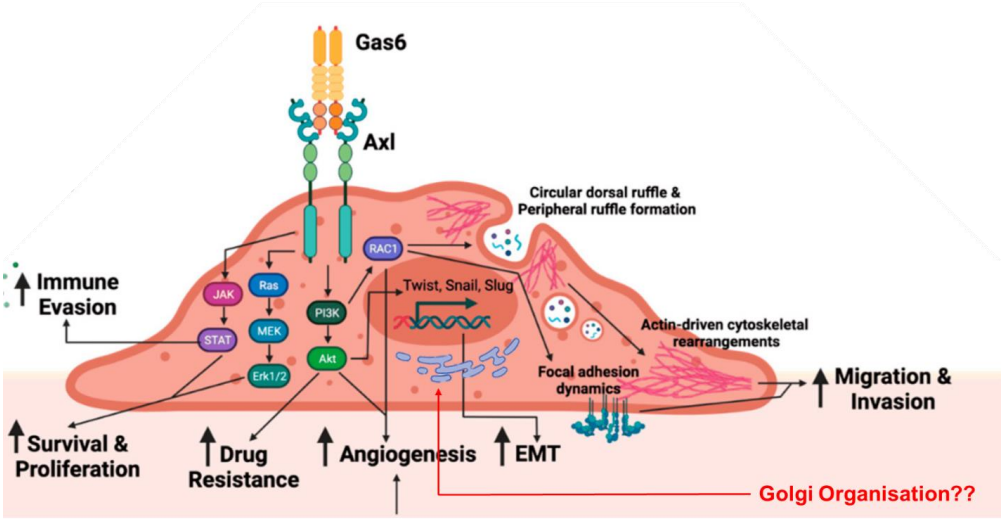

Figure 1.5: *AXL a receptor tyrosine kinase and its role in tumours.* (Paul and Mukhopadhyay, 2012)

Apart from this, there is also literature suggesting the role of AXL in Mechanosensing. This study (Yang et al., 2016) indicates a role for tyrosine kinases in cell mechanics. Here, they tried to understand the role of tyrosine kinases as Mechanosensing machines directly or indirectly. They found phospho-AXL and ROR2 localize to contraction units and bind major contractile components. After knocking down these RTKs (AXL and ROR2), altered rigidity sensing and increased duration of the local contraction units were found, respectively.

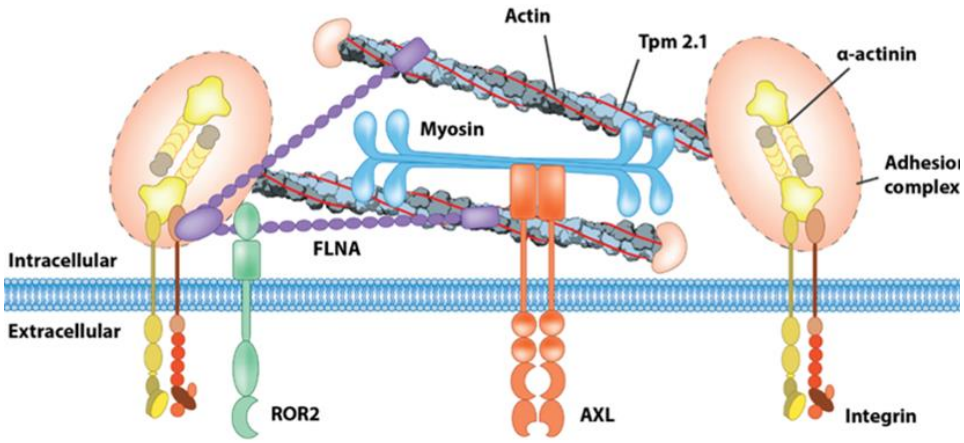

Figure 1.6: *AXL and ROR2 alter rigidity sensing and morphogenic processes by directly controlling local mechanosensory contractions without ligands.* (Yang et al., 2016)

Role of AXL in regulating the Golgi organization in MDAMB231:

The immunostaining of the AXL in MDAMB231 cells revealed that AXL distinctly localizes to the cis-Golgi (ManII-GFP) and trans-Golgi (GalT-RFP) markers (Unpublished data). Therefore, our approach was to ask a question in terms of the Golgi regulation in the two different cancer cells (MDAMB231 vs. MCF7), and this question can be addressed by targeting the AXL in the MDAMB231 cells to check its effect on the Golgi organization. This can be done by either inhibition or transient knockdown of the AXL. Their first approach is to use a small molecule inhibitor (R428) to target the AXL. R428 is a small molecule that acts as a specific and highly selective inhibitor of the AXL, which blocks the AXL's catalytic activity and the Akt's phosphorylation. R428 is currently in phase I/II clinical trials. This inhibition of the AXL caused the R428 concentration-dependent (0.5 µM, 1 µM, 2 µM) disorganization of the Golgi at population levels in MDAMB231 **(Unpublished data not shown)**. The reduction in the Akt activation (Ser473Akt) was confirmed at all concentrations of R428 to confirm the inhibition of the AXL.

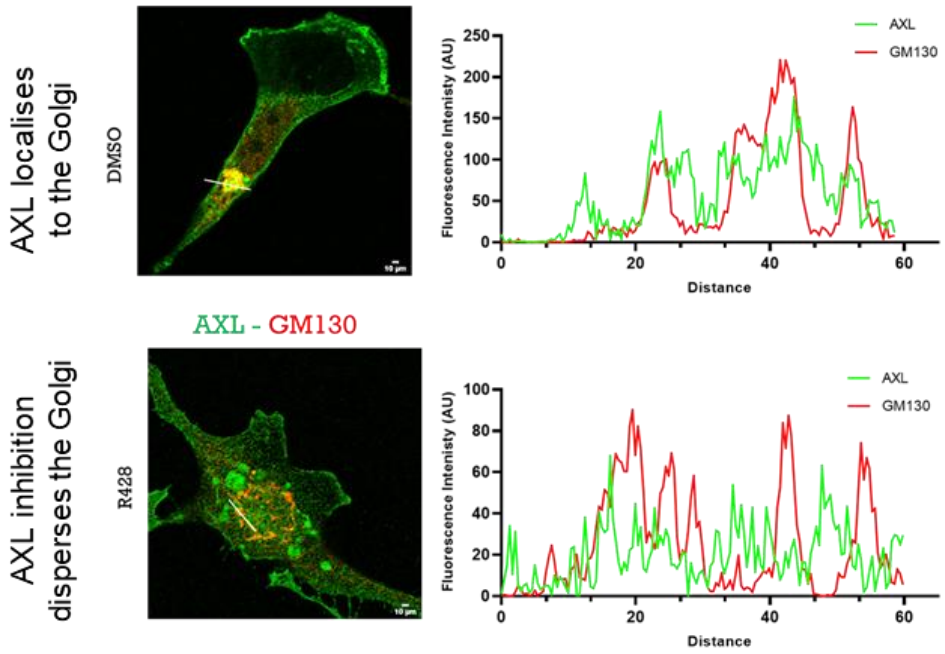

Figure 1.7: *Localisation of the AXL in control vs. R428 treated MDAMB231 cells. Red: GM130 and Green: AXL. Line intensity analysis was performed. Stable adherent cells show colocalization with the organised Golgi whereas R428 mediated inhibition of AXL causes the dispersal of the Golgi and the loss of AXL localisation from the Golgi as well. (unpublished data - Arnav Saha)*

AXL-Arf1 crosstalk regulates the Golgi organization:

Arf1 is a small GTPase known to regulate the Golgi organization and its function. Arf1, in its active form, gets associated with the Golgi membranes and gets released into the cytosol from the Golgi membranes (Donaldson et al., 2005). This activation of the Arf1 happens via GEFs (guanine nucleotide exchange factors) and GAPs (GTPase-activating proteins). This Arf1 is known to regulate the adaptors proteins, stacking or structural proteins on the Golgi membranes. Also, a previous study from the lab has established the essential role GTPase Arf1 has in the adhesion-dependent regulation of the Golgi organization in the anchorage-independent WT-MEFs (Singh et al., 2018). Hence, another study from the lab has tried to establish if this GTPase Arf1 has any role in the AXL-dependent regulation of the Golgi organization in the MDAMB231. This was explored by looking at the active status of the Arf1 (GGA3 pull-down assay) upon the R428 treatment, and a significant drop was observed in the Arf1 levels. Therefore, this drop in the active Arf1 levels could potentially contribute towards the AXL inhibition-mediated dispersal of the Golgi in MDAMB231.

It is also observed that GGA3 pull-down of the active Arf1 was seen to bring AXL with itself, which raises the possibility that the binding of the AXL and active Arf1 could contribute towards the regulation of the Golgi in MDAMB231 cells. The R428 treatment causes loss of AXL localization from the Golgi accompanied by the dispersal of Golgi. This could also cause the AXL-bound active form of Arf1 to be lost from the Golgi, leading to the Golgi disorganization. This data is also accompanied by expressing constitutively active Arf1 mutant-Q71L-mCherry constructs in the R428 treated MDAMB231, and results showed that there is predominantly organized Golgi in the population compared to the WT-Arf1-mCherry expressed cells in the background of R428 treatment. (Figure 1.7)

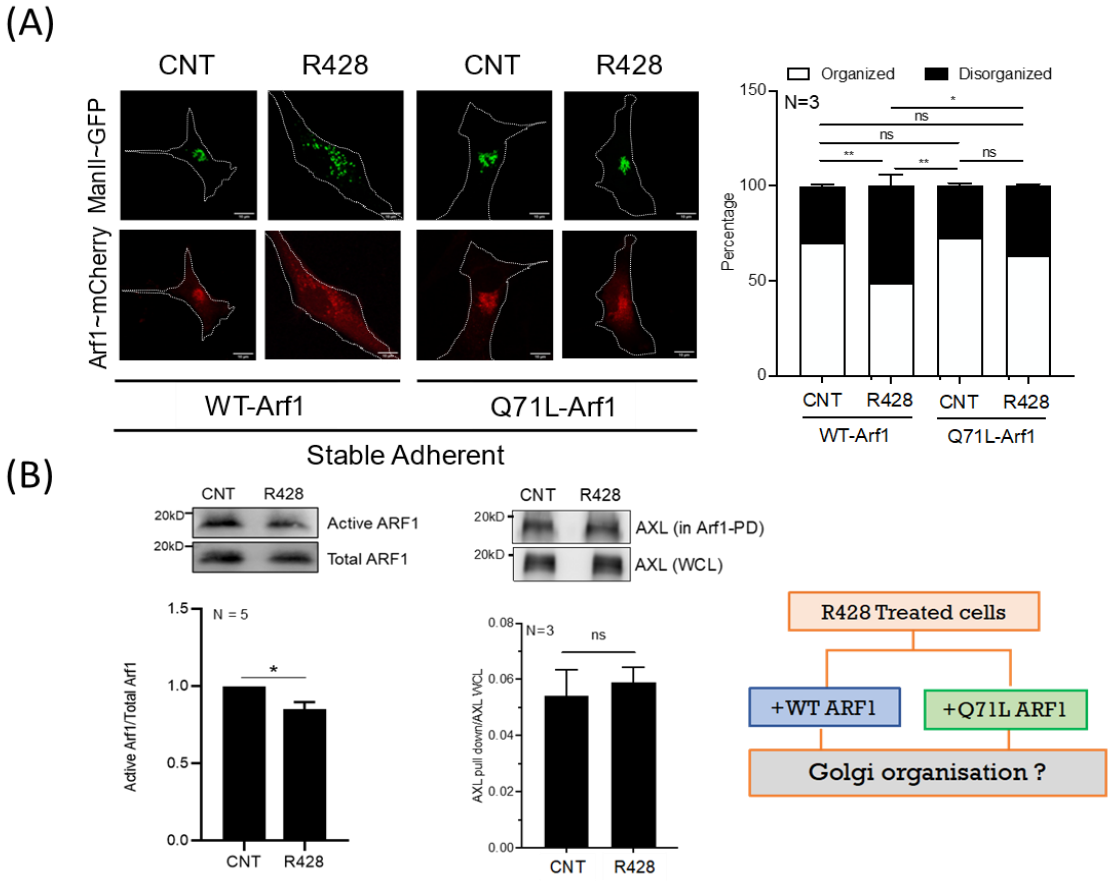

Figure 1.8: *(A) Effect of the Q71l-Arf1 expression on the Golgi organization in MDAMB231 cells upon R428 treatment. (B) Effect of the R428 treatment on the active Arf1 levels and the interaction of AXL and active Arf1. (unpublished data - Arnav Saha)*

Chapter 2: Materials and Methods

MATERIALS:

Antibodies:

Primary antibodies were diluted in the 5% BSA in TBST and used for the western blotting. The antibodies used are as follows: anti-AXL [Cell Signalling Technology, Danvers, MA, USA (CST), 3285] at 1:2000 dilution, Beta Tubulin [clone E7, Developmental Studies Hybridoma Bank, cat. No. AB_2315513] at 1:2000, Acetylated Tubulin [Sigma, St. Louis, MI, USA (Cat. No. T7451)] at 1:2000 and Arf1 [clone 1D9, Abcam, cat. No. ab2806] at 1:500. Also, the HRP-conjugated secondary antibodies [Jackson ImmunoResearch] were used at a dilution of 1:5000.

The following antibodies were used for the immunofluorescence assay: Anti-GM130 (BD Transduction, clone 35, cat. no. 610822) at a dilution of 1:100, Anti-AXL [Cell Signalling Technology, Danvers, MA, USA (CST), 3285] at 1:400 dilution. Secondary antibodies conjugated to Alexa Fluor 488 or Alexa Fluor 594 [Invitrogen Molecular Probes (cat. no. A12379 and A12381)] were used at a dilution of 1:1000.

Reagents:

The RIPA buffer used for the lysis of the cells is composed of the following things. 50 mM Tris/HCl pH 7.5 + 0.5% sodium deoxycholate + 0.05% SDS + 150 mM EDTA pH 8.0 + 1% NP40 + 150 mM NaCl. At the time of lysis using this RIPA buffer, PIC, 1 mM NaF and 1 mM NaO were added.

The following reagents were used to prepare the 2D hydrogels of varying stiffnesses. Acrylamide (HiMedia, Chennai, India, MB068), bisacrylamide (HiMedia, MB005), APS, TEMED (Sigma, T9281), MES buffer (Sigma, M8250), NHS (Sigma, 130672), EDC (Sigma, E1769), Toluene (Qualigens, Los Angeles, CA, USA, 32507), Silane (Sigma, 440159), Phalloidin-Alexa Fluor 488 (Invitrogen, A12379) at 1 : 400 dilution, DAPI (Invitrogen, D1306), Fluoromount-G (Southern Biotech, Birmingham, AL, USA, 0100-01), and Collagen (Gibco, Thermo Fisher Scientific, Waltham, MA, USA, Collagen I, Rat Tail, A1048301) were used.

Collagen [Gibco, Thermo Fisher Scientific, Waltham, MA, USA, Collagen I, Rat Tail, A1048301], fibronectin [Sigma, St. Louis, MI, USA (Cat. No. F2006)], and AXL inhibitor

named R428 [Cayman, USA (Cat. No. 21523)], Lipofectamine™ RNAiMAX Transfection Reagent [Invitrogen, USA (Cat. No. 13778150)] were also used.

All the plasmids used while performing the experiments are listed below. eGFP-AXL, ABD-GFP, ManII-GFP, GalT-RFP, pVSVG, pGagPol, AXL-pBABE puro, empty-pBABE puro and pMIG.

Cell culture:

Breast cancer cell lines MDAMB231 (M.D. Anderson Metastatic Breast) and MCF7 (Michigan Cancer Foundation-7) were cultured in complete Dulbecco's modified Eagle's medium (DMEM) (Invitrogen) with 5% fetal bovine serum (FBS) and penicillin-streptomycin (Pen-Strep; Invitrogen, Carlsbad, CA, USA) at 37°C in a 5% CO2 incubator. Trypsin was used to detach attached cells. Cells were routinely checked for mycoplasma contamination using DAPI staining.

Preparation of 2D hydrogels of varying matrix stiffnesses:

The 2D hydrogels of varying matrix stiffnesses were prepared using acrylamide solutions (40% acrylamide and 2% bisacrylamide) of varying concentrations in MiliQ. A similar height of the gels is ensured by taking an equal volume of the acrylamide solution. 45 µl drop was added on the nail-paint coated slide, and on top of that, a toluene-saline activated 12 mm rounded coverslip was kept and waited till it was polymerized (~ 20 mins). Then, these gels were washed with 1XPBS and treated with 0.1 M NGS-0.2 M EDC in MES buffer. These gels were overnight incubated at 4°C of 25 ug/ml collagen coating.

The next day, 10,000 cells were seeded on the gels and fixed after 24 hrs for MDAMB231 and MCF7. Then, it was stained with phalloidin A488 (1:300 dilution) and observed under EVOS FL auto-epifluorescence microscope at 20X objective. The areas of the cells were quantified using Fiji, an image analysis software.

Preparation of cell lysates from the 2D hydrogels of varying matrix stiffnesses:

To prepare the lysates of the cells seeded on the 2D hydrogels of varying matrix stiffnesses, 5 lakh cells were seeded on all stiffnesses (0.5kPa, 2.5kPa, 23kPa, Glass). After 24 hours of seeding, these cells spread on the 2D hydrogels were lysed using the RIPA buffer. At the time of lysis, PIC, 1 mM NaF and 1 mM NaO were added to RIPA buffer. All these reagents and all cell dishes were kept on ice to maintain the 4°C temperature. Take all the 2D hydrogels and put them in the new wells of 24 well plates so that the cells we are lysing are from only hydrogels, not the plastic plate around them. Then, gently add 20 µl of the RIPA buffer to the hydrogel and wait 15 minutes. Repeat this for two more times. After that, collect all the lysate from the wells, i.e., around the hydrogels, put them on top of the hydrogel, and mix gently for a few minutes. Collect all the lysates from the well into the 1.5 ml microcentrifuge tube and spin it at 10,000 rpm for 5 mins at 4°C.

Then, the BCA was done to estimate the protein amounts in the collected lysate. Once the required amount of lysate was taken for BCA, the Lamelli was added to the RIPA lysates, then mixed well and boiled at 95°C at 500 rpm for 15 minutes. These lysates were stored at the -20°C till further use.

AXL inhibition using R428:

After 24 hrs of cell seeding on 2D hydrogels/ glass, R428 treatment was done on MDAMB231 cells for 12 hrs by adding the appropriate volume of the inhibitor in the culture medium so that the final concentration of R428 is 1 µM. R428 was reconstituted in DMSO, and hence same volume of DMSO was added to the culture media for the control condition.

siRNA-mediated knockdown of AXL:

After 24 hrs of MDAMB231 cell seeding, two consecutive transfection shots were done using RNAi max of both siAXL#1 and siAXL #2 (50 pmol siRNA was used). The first shot was after 24 hrs of seeding, and the second one after 24 hrs of the first

transfection shot. Then, cells were allowed to stay with media containing the transfection mix for another 48 hrs. After that, these cells were seeded on the collagen-coated 2D hydrogels/ glass and were allowed to grow for 24 hrs. Remaining equal volumes of cell suspension (approx. same cell number) were plated on 60 mm plastic dishes for preparing lysates to validate using western blotting. This was to check for the efficiency of the AXL knockdown in MDAMB231 cells using both the siRNAs.

Transfection of plasmids:

Transfection in MCF7 was done using 6 µl PEI (Polyethyleneimine) and 2 µg plasmid DNA on 5 lakh cells (in 6 cm dishes) after 24 hrs of seeding. For MDAMB231, transfection was done using 3 µl of lipofectamine 2000 (a transfecting reagent) and 3 µg of plasmid DNA (ManII-GFP & GalT-RFP) after 24 hrs of seeding. After every 12 hrs post-transfection, transfection efficiency was checked up to 48 hrs. After 48 hrs, cells were replated on a fibronectin-coated coverslip for 24 hrs. They were stained with DAPI after fixing with 3.5% PFA before mounting on a glass slide using mounting medium Fluoromount-G.

Immunofluorescence Assay:

After 24 hrs of cell seeding on 2D hydrogels/ glass where cells have spread, they were fixed using the 3.5% PFA (paraformaldehyde) for 15 mins. Then, cells were incubated in 0.5% Triton-X in 5% BSA in 1XPBS for 10 mins; further, blocking was done for 1 hr at RT using 5% BSA in 1XPBS. After blocking, cells were incubated overnight for anti-GM130 primary antibody (1:100 dilution in 5% BSA in 1XPBS). After 12 hrs of primary antibody incubation, the anti-mouse secondary antibody (A568) was incubated against GM130, and DAPI staining was also done. These 2D hydrogels were mounted using the mounting medium Fluoromount-G.

The Golgi organization distribution profile was imaged using an EVOS M7000 Invitrogen microscope with a 100X oil emulsion objective. The following parameters were used for imaging in the confocal microscope. (Parameters: The 'best signal' option from the smart setup. A488 (or EGFP), A568 and DAPI channels were chosen. Frame size- 1024 X 1024, speed- 5, averaging number- 4, unidirectional scanning,

zoom- 2, airy units- 1 AU, Gain (Master)- 600 to 800, digital offset- 1, signal intensity has been adjusted using the function range indicator.

Actin staining:

The fixed cells on glass coverslips or 2D hydrogels were incubated in the Phalloidin-Alexa Fluor 488 at 1:100 dilution for 12 hrs for 2D hydrogels at 4°C inside the humid chamber.

SDS-PAGE and Western blotting:

Cells were lysed using the 200 µl 1X Lamelli buffer in a 60 mm dish. Lysates were run using SDS-PAGE (with 5% stacking gel and 12.5% resolving gel) with running buffer (containing 100 ml 10X Tris-glycine, 10 ml 10% SDS and 890 ml distilled water) at a constant volt of 30 V (15 mA current) for the first 30 min to get proteins into the resolving gel and then at 120 V for next 1.5 hrs (till dye flows out of polyacrylamide gel). Then, the transfer proteins to the PVDF membrane for 2 hrs in chilled transfer buffer (Transfer buffer composition: 100 ml 10X Tris-glycine, 100 ml methanol, 800 ml distilled water and 1 ml 10% SDS). Then, the PVDF membrane was blocked with 5% milk diluted in 1XTBST for an hour, and then 1° antibody incubation was done for 12 hrs. The next day, after giving 3 washes of 1XTBST each of 10 min, the blot was incubated in the 2° antibody for 1 hr, and again, three washes with 1XTBST were given. Finally, a blot was developed in the ImageQuantTM LAS 4000 system using substrate and luminol (in the 1:1 ratio) solution.

Making stably AXL expressing MCF7 cells using retroviral transduction:

1.5 lakh HEK293T cells were seeded in the 6 cm dish. Such 3 dishes were made. After 24 hrs, transfection of plasmids was done in all three dishes, in combination, as shown in Figure 3B. One dish for transducing AXLpBABEpuro, another for transducing empty-pBABEpuro and the third one for pMIG were used. Wait for 48 hrs to add 10%

DMEM. At the same time, seed 1.5 lakh MCF7 cells each in three 35 mm dishes. Then, after 24 hrs, collect the viral titter, filter it using the 0.2 microns filter and add it in the MCF7 cells (confluency of MCF7 cells should be approximately 50%, as we are using retroviral vector) with the following combination: 3 ml viral titter and 1 ml 10% DMEM with 4 µl of 10 µg/ml polybrene. After 72 hrs of the viral titer addition, puromycin selection is started. The final working concentration of the puromycin in the cell medium is 1.6 µg/ml. Track the cell viability every 24 hrs post addition of the puromycin for another 72 hrs. After 72 hours, if transduction has worked, there should be visible colonies that have not died. Give 1XPBS wash thrice to remove the dead cells and the excess debris, and replate these cells into the wells of 24 well plates to allow them to grow. Once the well gets confluent, split it into the two wells of 24 well plates and will enable them to grow again.

Here, pMIG (a retroviral vector with the GFP-tag) is used as a positive control to check the transfection efficiency in HEK293T and transducing efficiency in the MCF7 after adding the viral titter.

Microscopy Imaging and Image Analysis:

Images for calculating the cell spreading of the cells stained for actin were captured on the 20X air objective of EVOS FL Auto Imaging System (Thermo Fisher, Waltham, MA, USA, AMAFD100).

Also, Golgi and AXL staining images were captured at the confocal microscope, and the following parameters were set up. The best signal option has been chosen from the smart setup. Frame size - 1024 X 1024, speed – 5, averaging no. – 4, scanning directionality is kept unidirectional, zoom – 2, airy units – 1 AU, Gain (Master) – 600 to 800, digital offset -1, sample and background signal intensity has been adjusted using the range indicator. Cell-spread area, aspect ratio analysis and Golgi object-count analysis were performed using the Fiji software, NIH, Bethesda, MA, USA.

Statistical Analysis:

All the statistical analysis was done using the GRAPHPAD PRISM software, San Diego, CA, USA. Data was analyzed using the two-tailed, unpaired, nonparametric Mann-Whitney test for non-normalized data and single sample t-test for normalized data. Statistical significance was assigned as: * $p < 0.05$, ** $p < 0.01$, *** $p < 0.001$, **** $p < 0.0001$.

Chapter 3: Results and Discussions

3.1: Differential Golgi organization of MDAMB231 vs MCF7 cells on varying matrix stiffnesses accompanied by differential cell spreading.

A preliminary screen was performed in our lab to establish the Golgi profile of anchorage-independent cancer cell lines of different origins. The breast cancer cell line pair, MCF7 and MDAMB21, from that preliminary screen revealed contrastingly different Golgi phenotypes. MDAMB231, a triple-negative breast cancer cell line, had a predominant organized/compact Golgi phenotype, whereas MCF7 showed a disorganized phenotype in a stably adherent state (Figure 3.1 A). Another aspect we were interested in looking at was whether the Golgi profile of these cell lines changes upon loss of cell-ECM adhesion. Previous works from the lab had established that the Golgi dramatically disorganizes upon loss of adhesion in normal anchorage-dependent cell lines like mouse and human fibroblasts. The breast cancer cell line pair of MDAMB231 and MCF7 show a unique regulation on loss of cell-ECM adhesion, as the Golgi is distinctly disorganized in MDAMB231 while in MCF7, the Golgi remained disorganized upon loss of adhesion (Fig 3.1 A) *(unpublished data - Prachi Joshi, Arnav Saha).* This distinct phenotype was validated using Cis (ManII-GFP) and Trans (GalTase-RFP) Golgi markers. This data revealed that MDAMB231 has an anchorage-dependent regulation of Golgi, while in MCF7 cells this regulation is anchorage-independent.

Breast cancer cells are known to respond to mechanical cues, through the regulation of integrin-mediated adhesion. The following preliminary data led us to ask if matrix stiffness could regulate the Golgi in MDAMB231 and MCF7 cells. This also aims to answer a vital question, on if endomembrane organelles like the Golgi can sense physical cues like stiffness and whether the structural organization of the Golgi and its functions are affected by matrix stiffness.

The first aim for this thesis was to characterize Golgi organization of MDAMB231 cells seeded on PA-gels of varying matrix stiffness (0.5 kPa, 2.5 kPa, 23 kPa, glass) coated with collagen (25 µg/ml). When MDAMB231 cells were seeded on matrices of varying stiffnesses they showed a predominantly disorganized Golgi organization on the lower stiffnesses (0.5 kPa and 2.5 kPa).

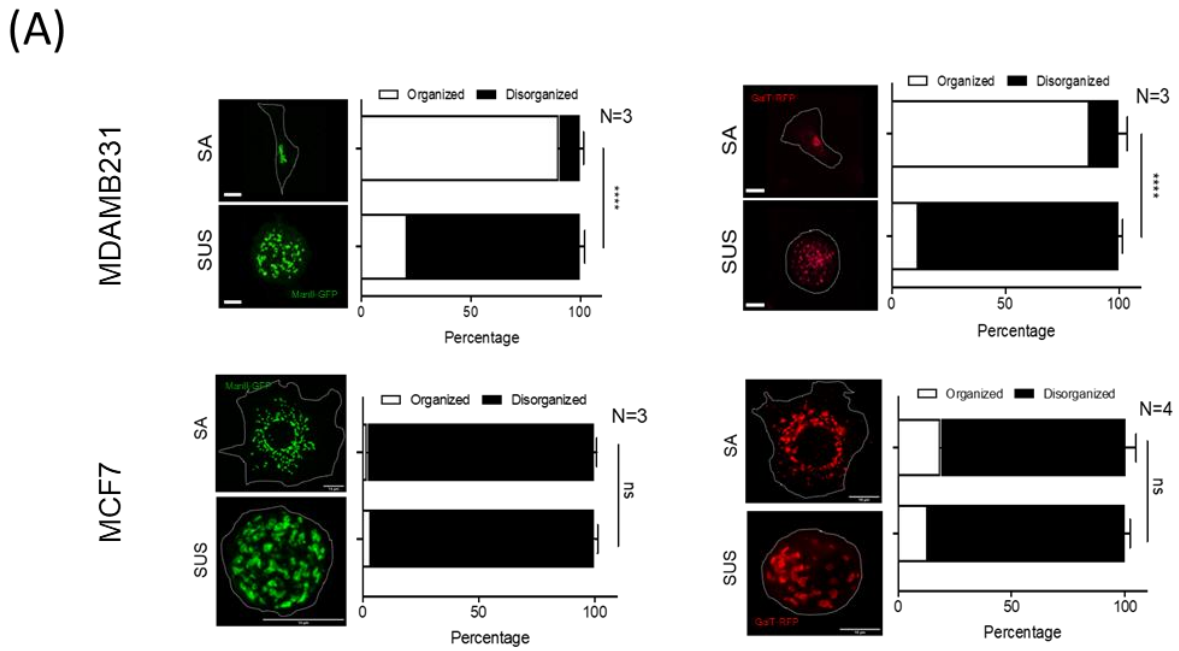
(A)
MDAMB231
MCF7
SA
SUS
Organized
Disorganized
N=3
N=4
****
ns
Percentage
0
50
100
GalT-RFP
ManII-GFP

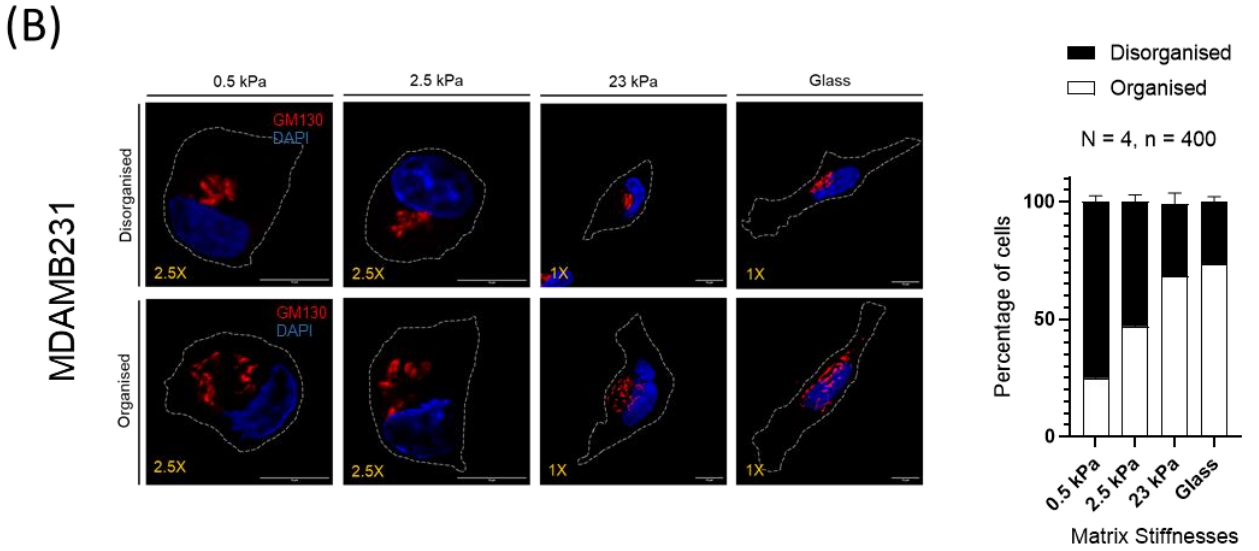
(B)
MDAMB231
0.5 kPa
2.5 kPa
23 kPa
Glass
Disorganised
Organised
GM130
DAPI
2.5X
1X
Disorganised
Organised
N = 4, n = 400
Percentage of cells
100
50
0
0.5 kPa
2.5 kPa
23 kPa
Glass
Matrix Stiffnesses

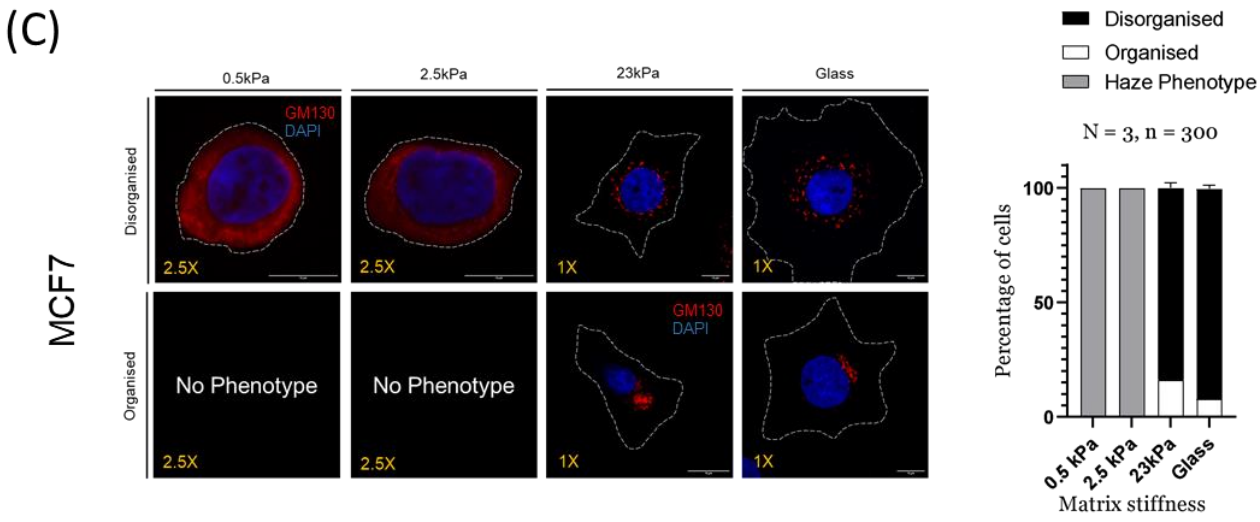
(C)
MCF7
0.5kPa
2.5kPa
23kPa
Glass
Disorganised
Organised
GM130
DAPI
No Phenotype
2.5X
1X
Disorganised
Organised
Haze Phenotype
N = 3, n = 300
Percentage of cells
100
50
0
0.5 kPa
2.5 kPa
23kPa
Glass
Matrix stiffness

(D)

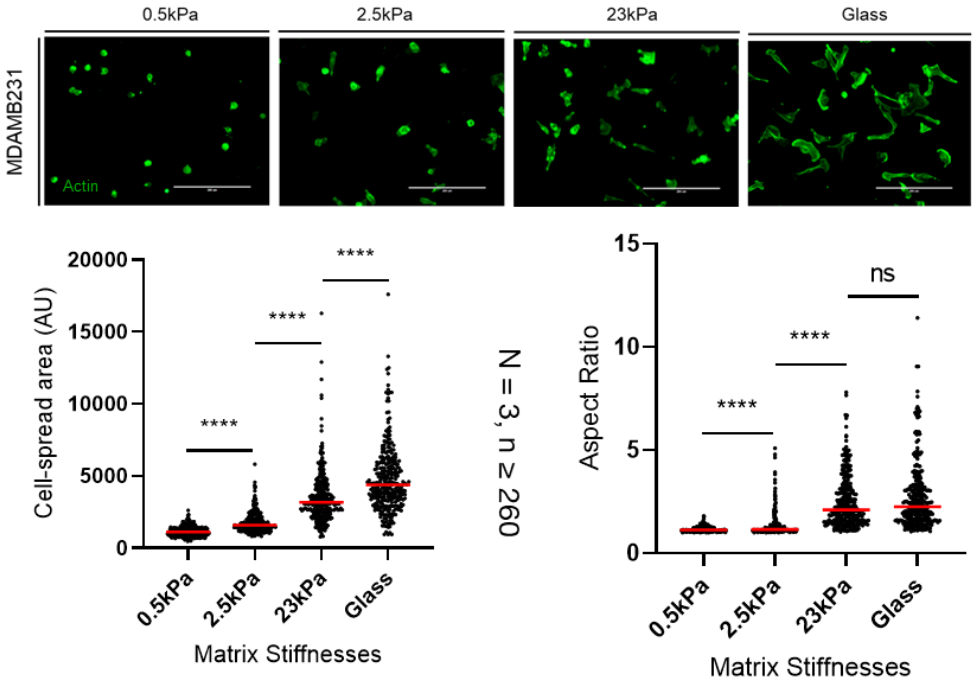
0.5kPa
2.5kPa
23kPa
Glass
MDAMB231
Actin
Cell-spread area (AU)
20000
15000
10000
5000
0
****
****
****
0.5kPa
2.5kPa
23kPa
Glass
Matrix Stiffnesses
N = 3, n ≥ 260
Aspect Ratio
15
10
5
0
****
****
ns
0.5kPa
2.5kPa
23kPa
Glass
Matrix Stiffnesses

(E)

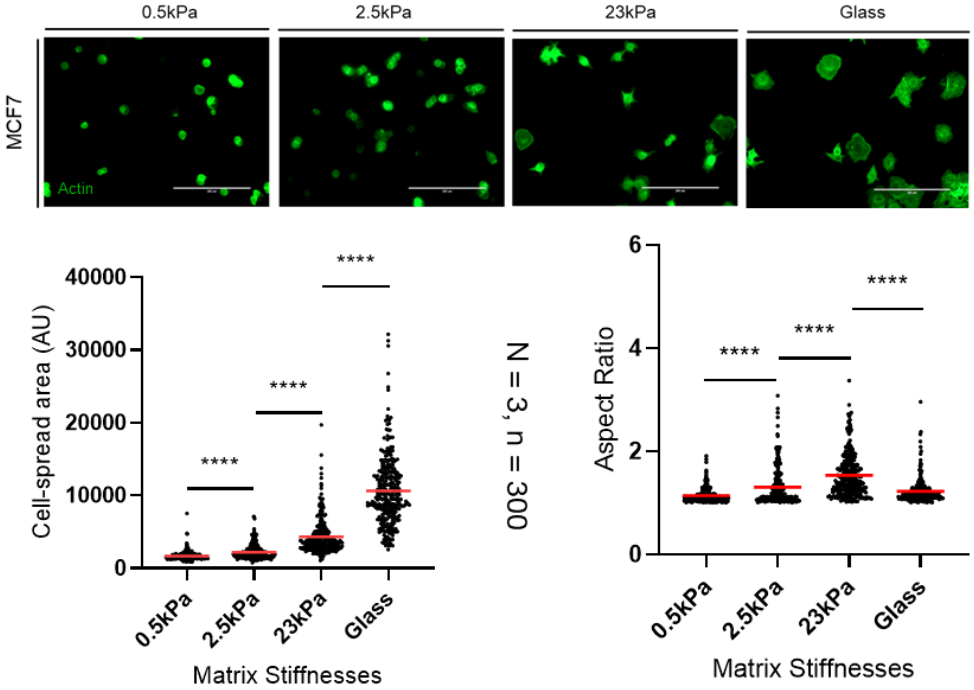
0.5kPa
2.5kPa
23kPa
Glass
MCF7
Actin
Cell-spread area (AU)
40000
30000
20000
10000
0
****
****
****
0.5kPa
2.5kPa
23kPa
Glass
Matrix Stiffnesses
N = 3, n = 300
Aspect Ratio
6
4
2
0
****
****
****
0.5kPa
2.5kPa
23kPa
Glass
Matrix Stiffnesses

(F)

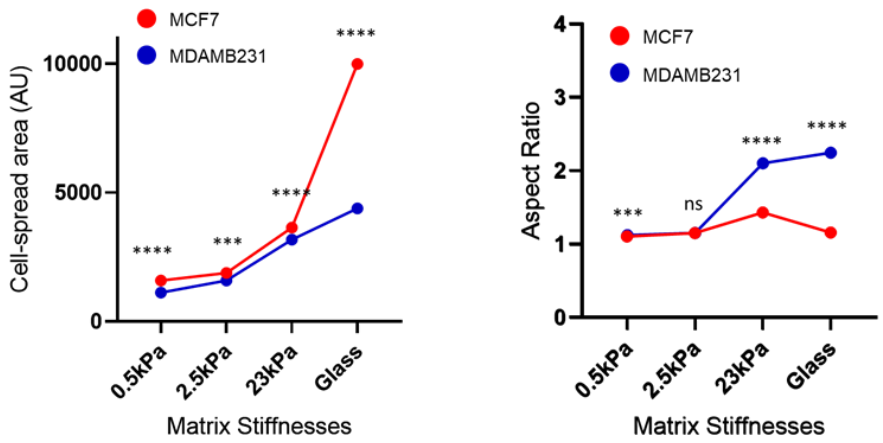
MCF7
MDAMB231
Cell-spread area (AU)
10000
5000
0
****
***
****
****
0.5kPa
2.5kPa
23kPa
Glass
Matrix Stiffnesses
MCF7
MDAMB231
Aspect Ratio
4
3
2
1
0
***
ns
****
****
0.5kPa
2.5kPa
23kPa
Glass
Matrix Stiffnesses

Figure 3.1: *Characterisation of the Golgi phenotypes in stable adherent (SA) vs. suspension (SUS) in MDAMB231 and MCF7 cells. Similarly, characterisation of the Golgi phenotypes and cell spreading on 2D hydrogels of varying matrix stiffnesses for MDAMB231 and MCF7 cells. Staining was done using the anti-GM130 antibody (Golgi) and phalloidin Alexa flour-488 (actin). (A) These cells were transfected with the Golgi markers (ManII-GFP and GalT-RFP) to look at the Golgi organization. The graph next to the figures represents the percentage of cells showing organized or disorganized Golgi phenotype and distribution profile in SA vs. SUS. (Unpublished data - Prachi Joshi, Arnav Saha) (B). Images depict the Golgi organization phenotypes at the respective stiffnesses, and the graph next to them shows the Golgi organization distribution profile for MDAMB231 cells. (C) Representative images and Golgi organization distribution profile for MCF7 cells. (D) Images represent the spreading of the cells, and the graphs next to them represent the spread area and aspect ratio of MDAMB231 cells on matrices of varying stiffness. (E) Representative images and quantitation of cell-spread area and aspect ratio for MCF7 cells. (F) Comparison of cell-spread area and aspect ratio between the MDAMB231 and MCF7 cells.*

In contrast, Golgi organization was predominantly organized on higher stiffnesses, i.e., 23 kPa and Glass (Figure 1B, 1C). In the case of MCF7 cells, when seeded on the varying matrix stiffnesses, the predominant Golgi phenotype remains disorganized on higher stiffnesses (23 kPa and Glass). On lower stiffnesses (0.5 kPa, 2.5 kPa), the Golgi phenotype is distinctly different from the usual organized and disorganized Golgi organization. The Golgi labelled with GM130 is largely diffused throughout the cytosol in these cells. No distinct Golgi objects were visible leading us to speculate that this phenotype can be unique fragmentation of the Golgi. Further evaluation of this phenotype with other markers will be of interest in understanding if this phenotype is unique to MCF7 or is seen in other cell types.

In breast cancers, tumour stiffening is a well-characterized feature of cancer progression. Normal breast tissue usually has a stiffness ranging from 0.5 to 2.5 kPa. However, breast tumour tissue shows a heterogenous stiffness distribution ranging from 0 to 20 kPa (Liu et al.). Though both MDAMB231 and MCF7 are breast cancer cell lines, they are known to be significantly different in terms of characteristics like tumour subtype, hormone receptor presence, EMT status, and characteristic metabolism (Theodossiou et al.). Hence, we also wanted to establish if these two cell lines could differentially respond to varying matrix stiffnesses relative to each other, by evaluating their ability to spread on changing matrix stiffness.

Both MDAMB231 and MCF7 cells, when seeded on collagen-coated-2D polyacrylamide gels of 2.5 kPa (Soft) and 23 kPa (Stiff), showed an increase in cell spreading area (detected by phalloidin staining) with an increase in stiffness of the matrix (Figure 1D, 1E). The non-physiological stiffness of glass provides a valuable control for cells cultured in lab conditions. This suggested that both these cell lines are mechanosensitive and respond to changing substrate stiffness. Although both these cell lines are mechanoresponsive, when the cell-spread area of these two cell lines is compared, the MCF7 cell spread more than MDAMB231 (Figure 1F). This difference gets more prominent as we shift to the stiffer matrices. This led us to further investigate if a how aspect ratio of these two cell lines is affected by varying matrix stiffnesses. This would be an effective readout of whether the cellular polarity is also affected by matrix stiffness in these two breast cancer cells types. The main reason for looking at cell polarity is to establish links between changes in cellular polarity and cell spreading, which could affect the organization of endomembrane organelles like the Golgi. The Golgi apparatus is known to act as a signalling hub to regulate cell polarity (Ravichandran et al., 2020); hence, changes in cellular polarity could be a direct consequence of the Golgi organization's being affected by changing matrix stiffness or vice versa. The actin and microtubule cytoskeleton network regulate the assembly of the Golgi ribbon and also the positioning and the maintenance of the Golgi apparatus for the cell motility and the polarised cell trafficking (Copeland et al.). Hence, could differentially spreading of the cells on varying matrix stiffnesses connect to the regulation of the Golgi organisation in stiffness dependent manner is worth checking.

The aspect ratio was quantified by calculating the ratio of the major to the minor axis of the ellipse fit to the cell, which means the more significant the aspect ratio, the more cellular polarization. MDAMB231 cell shows an increasing trend in aspect ratio as the matrix stiffness increases, indicating cellular polarity is regulated by matrix stiffness. Meanwhile, MCF7 cells show a significant increase in their polarisation on 23 kPa stiffness compared to all other stiffnesses. However, the aspect ratio remained considerably low and comparable in lower stiffness (0.5 kPa, 2.5 kPa). This was interestingly comparable to aspect ratio seen on Glass. This was another exciting observation concerning how these cells differentially behave, as although both are mechanoresponsive, they do not show similar trends in cellular polarity. The role Golgi

organisation could have in mediating the same remains of particular interest to test further.

3.2: Effect of AXL inhibition and AXL Knockdown on Golgi organization and cell spreading across varying matrix stiffness in MDAMB231 cells.

As discussed, our lab has established that AXL can act as a vital payer of Golgi organization and functions via regulating the activation and localization of the Arf1 GTPase. We wanted to extend this further by understanding whether AXL has any role in mediating the mechano-responsiveness of MDAMB231 and MCF7 and the impact its regulation of the Golgi organization could have in mediating it. An earlier study also reported that the AXL receptor has a role in cellular rigidity sensing with active phospho-AXL seen to localize to actomyosin contractile units (Yang et al., 2016). Hence, we aimed to test whether AXL has any role in the stiffness-dependent regulation of Golgi organization in MDAMB231 and MCF7. We started working on MDAMB31 cells with very high AXL expression to test this hypothesis. As discussed previously, experiments in the lab tested the AXL-specific inhibitor R428 to understand its role in Golgi organization and functions. When the inhibitor was tested across a concentration range (0.5, 1, and 2 µM) on MDAMB231 cells, the Golgi showed significant disorganization at 1 and 2 µM concentrations. This suggests that AXL activation could regulate Golgi organisation. For our further studies, we used 1 µM R428 as it is the lowest concentration which significantly affected Golgi phenotype. We further wanted to check what happens to Golgi organization of MDAMB231 cells seeded on the matrices of varying stiffnesses in the presence and absence of the AXL inhibitor. From Figure 1B, a matrix stiffness-dependent regulation of the Golgi organization in MDAMB231 cells could be concluded. When MDAMB31 cells seeded on the varying matrix stiffnesses were treated with the R428 (1uM), the stiffness-dependent regulation of the Golgi organization was found to be perturbed entirely on all stiffnesses (Figure 2A). This was a very striking observation as it suggests the need for that further evaluation on whether AXL expression and activation are regulated by stiffness. It also supports the possibility that AXL activation

status could have a role in regulating Golgi organization as cells respond to ECM properties like stiffness.

As this was a very striking observation that implied that AXL is a vital player in the stiffness-dependent regulation of Golgi organization in MDAMB231 cells, the best way to confirm this was to perform an AXL-knockdown and see how it affects this stiffness-dependent regulation of Golgi organization. AXL knockdown was performed using two siRNAs (siAXL#1 and siAXL#2). The knockdown efficiency using both the siRNAs was validated by performing western blotting to check the effect on total AXL levels (Figure 3.2 H). We observed approximately 80% reduction in total AXL levels upon knockdown using either siRNAs (Figure 3.2 H). We also evaluated whether AXL knockdown affects total Arf1 levels, as we are particularly interested in evaluating the AXL-Arf1 crosstalk to what happens in changing matrix stiffness. Our observations revealed that AXL knockdown does not significantly affect total Arf1 levels (Figure 3.2 H). AXL knockdown MDAMB231 cells (using siAXL#1 and siAXL#2) distinctly disrupted the stiffness-dependent regulation of Golgi organization observed in control cells. This when quantified by the distribution profile of the Golgi organization, revealed the Golgi to be predominantly disorganized across all stiffnesses (Figure 2B). Our observations with both the AXL inhibitor and AXL knockdown confirms AXL levels and activation to be crucial in determining the stiffness-dependent regulation of Golgi organization in MDAMB231 cells. Further studies are needed to understand how AXL regulates this stiffness-dependent Golgi organization in MDAMB231 cells. Our future experiments will evaluate AXL activation status and localization in cells on matrices of varying stiffness. We also aim to assess if and how the AXL-Arf1 crosstalk could be relevant in this matrix stiffness-dependent regulation of Golgi organization.

AXL, a receptor tyrosine kinase, is predominantly present on the plasma membrane, has crosstalk with various other cell surface receptors, and has been shown to regulate actin cytoskeletal dynamics. The GAS6-AXL signalling cascade induces multiple actin-driven cytoskeletal rearrangements, contributing to cell invasion in cancers (Zdzalik-Bielecka et al., 2021). The actin-cytoskeletal network also has well-established links with the organization, rheology, and various functions of the Golgi apparatus, like trafficking and metabolism (Phuyal et al., 2023). Few studies have

Figure 2

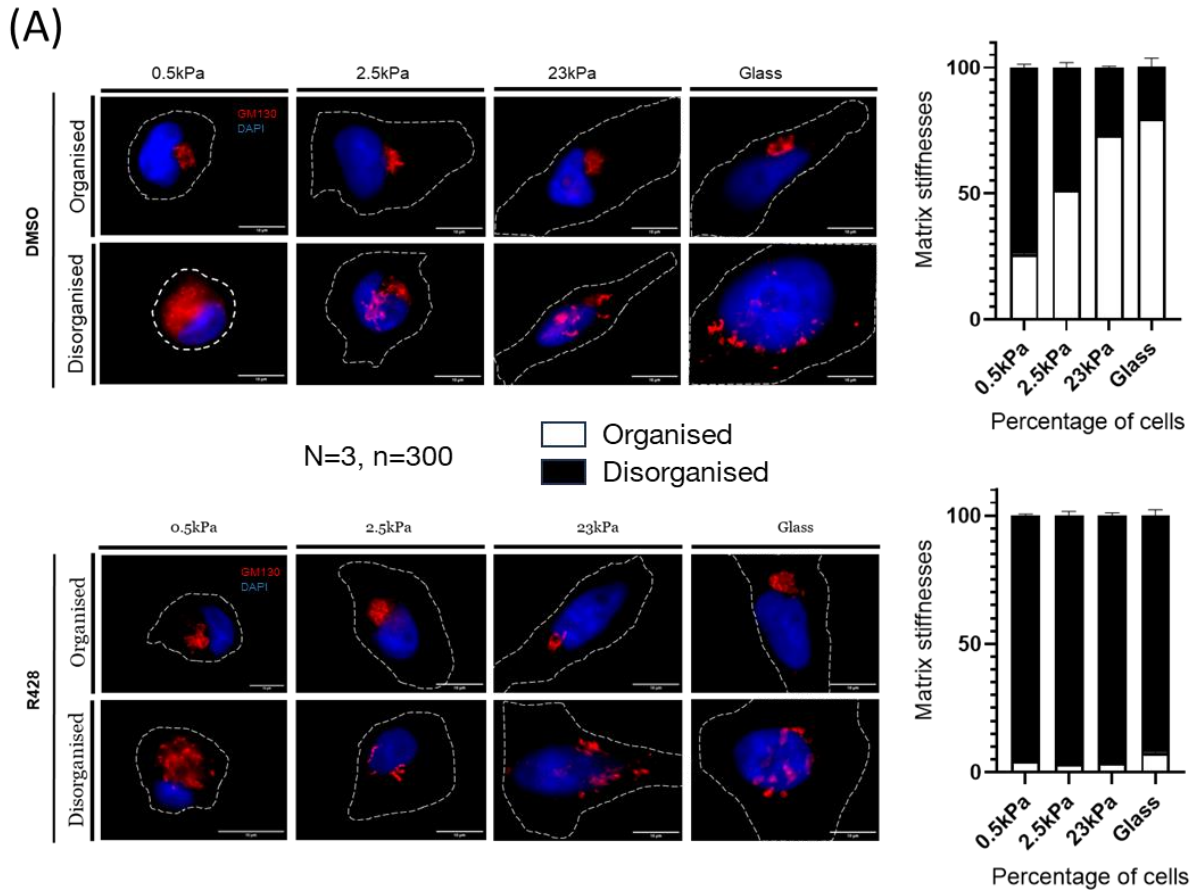
(A)
0.5kPa
2.5kPa
23kPa
Glass
DMSO
Organised
Disorganised
GM130
DAPI
Matrix stiffnesses
100
50
0
0.5kPa
2.5kPa
23kPa
Glass
Percentage of cells
N=3, n=300
Organised
Disorganised
R428
Organised
Disorganised
GM130
DAPI
Matrix stiffnesses
100
50
0
0.5kPa
2.5kPa
23kPa
Glass
Percentage of cells

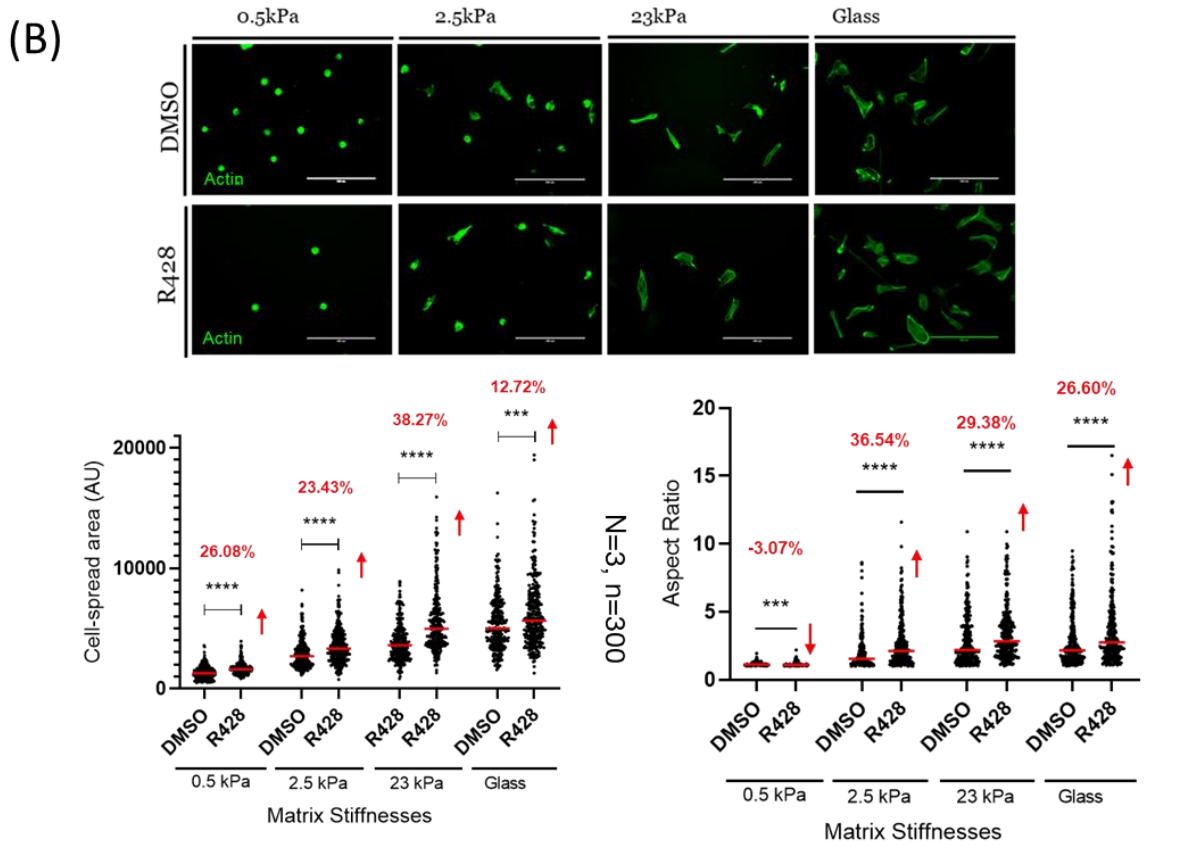
(B)
0.5kPa
2.5kPa
23kPa
Glass
DMSO
Actin
R428
Actin
Cell-spread area (AU)
20000
10000
0
26.08%
****
23.43%
****
38.27%
****
12.72%
***
DMSO
R428
DMSO
R428
R428
R428
DMSO
R428
0.5 kPa
2.5 kPa
23 kPa
Glass
Matrix Stiffnesses
N=3, n=300
Aspect Ratio
20
15
10
5
0
-3.07%
***
36.54%
****
29.38%
****
26.60%
****
DMSO
R428
DMSO
R428
DMSO
R428
DMSO
R428
0.5 kPa
2.5 kPa
23 kPa
Glass
Matrix Stiffnesses

(C)

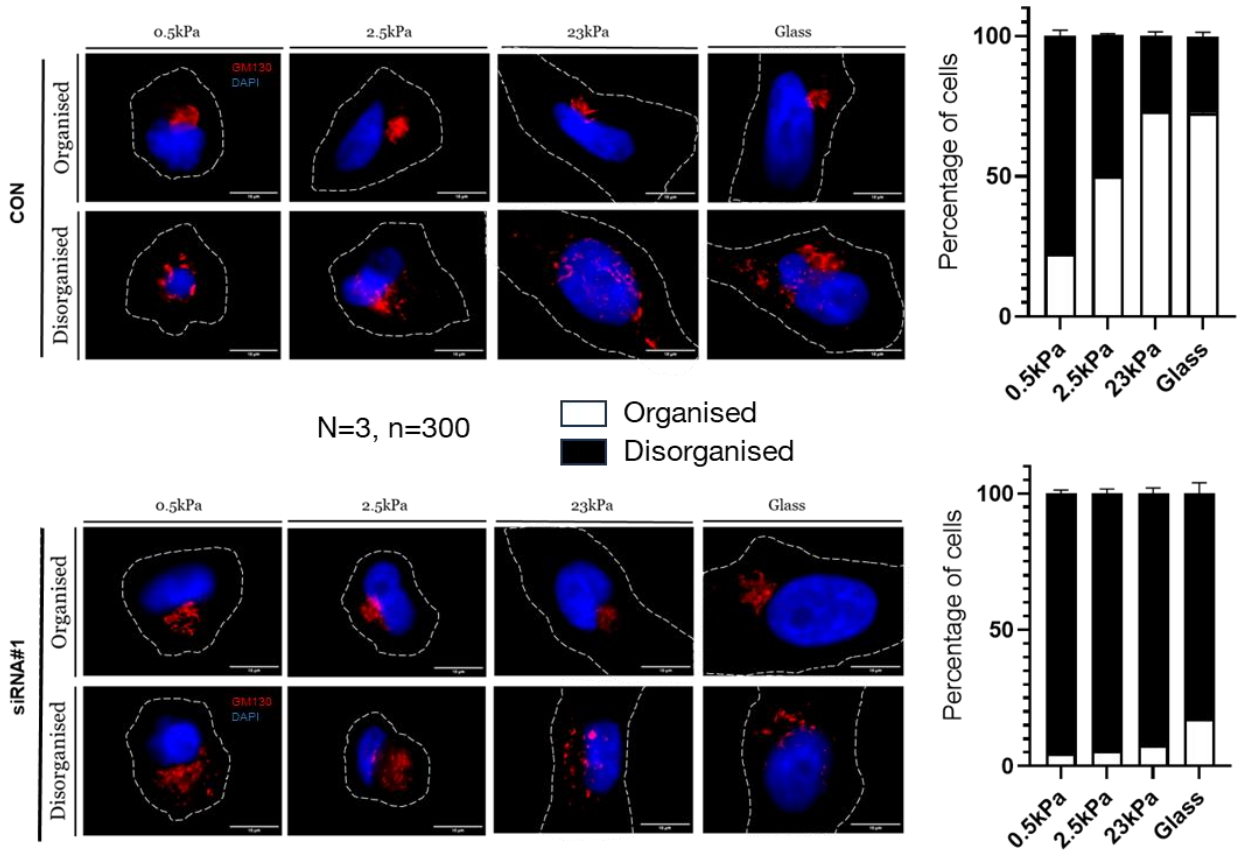
0.5kPa
2.5kPa
23kPa
Glass
CON
siRNA#1
Organised
Disorganised
GM130
DAPI
Percentage of cells
100
50
0
N=3, n=300
Organised
Disorganised

(D)

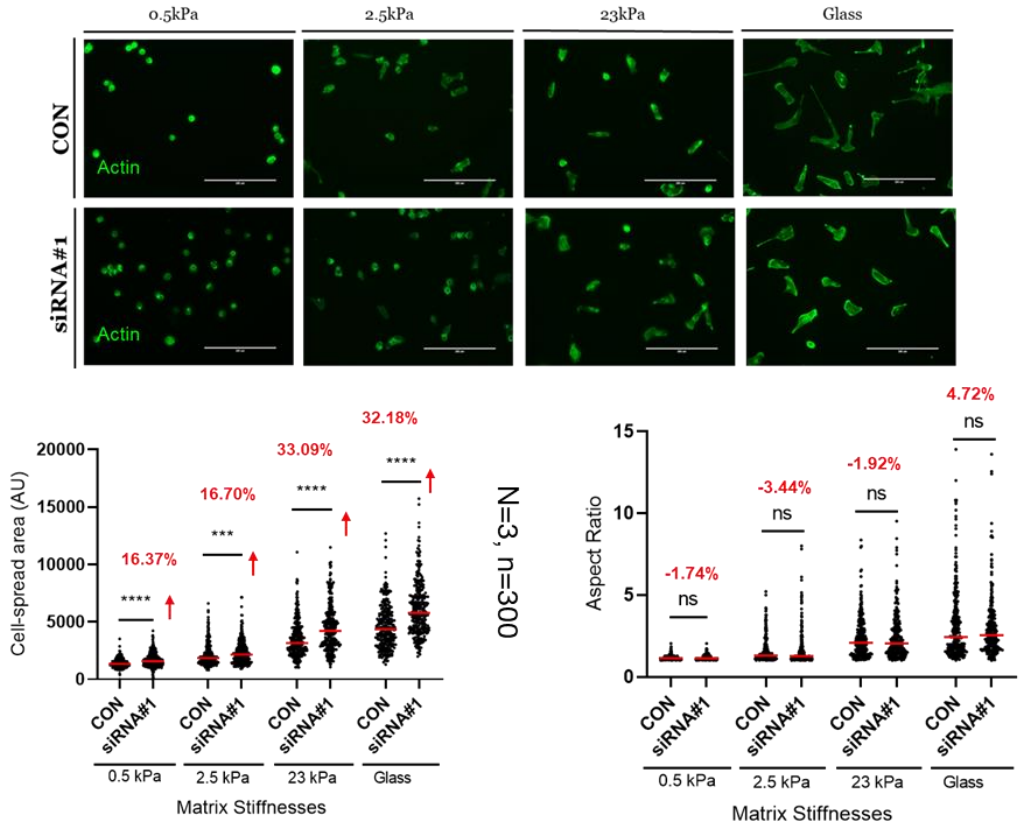
0.5kPa
2.5kPa
23kPa
Glass
CON
siRNA#1
Actin
Cell-spread area (AU)
20000
15000
10000
5000
0
16.37%
16.70%
33.09%
32.18%
****
***
****
****
N=3, n=300
Aspect Ratio
15
10
5
0
-1.74%
-3.44%
-1.92%
4.72%
ns
ns
ns
ns
CON
siRNA#1
0.5 kPa
2.5 kPa
23 kPa
Glass
Matrix Stiffnesses

Figure 2

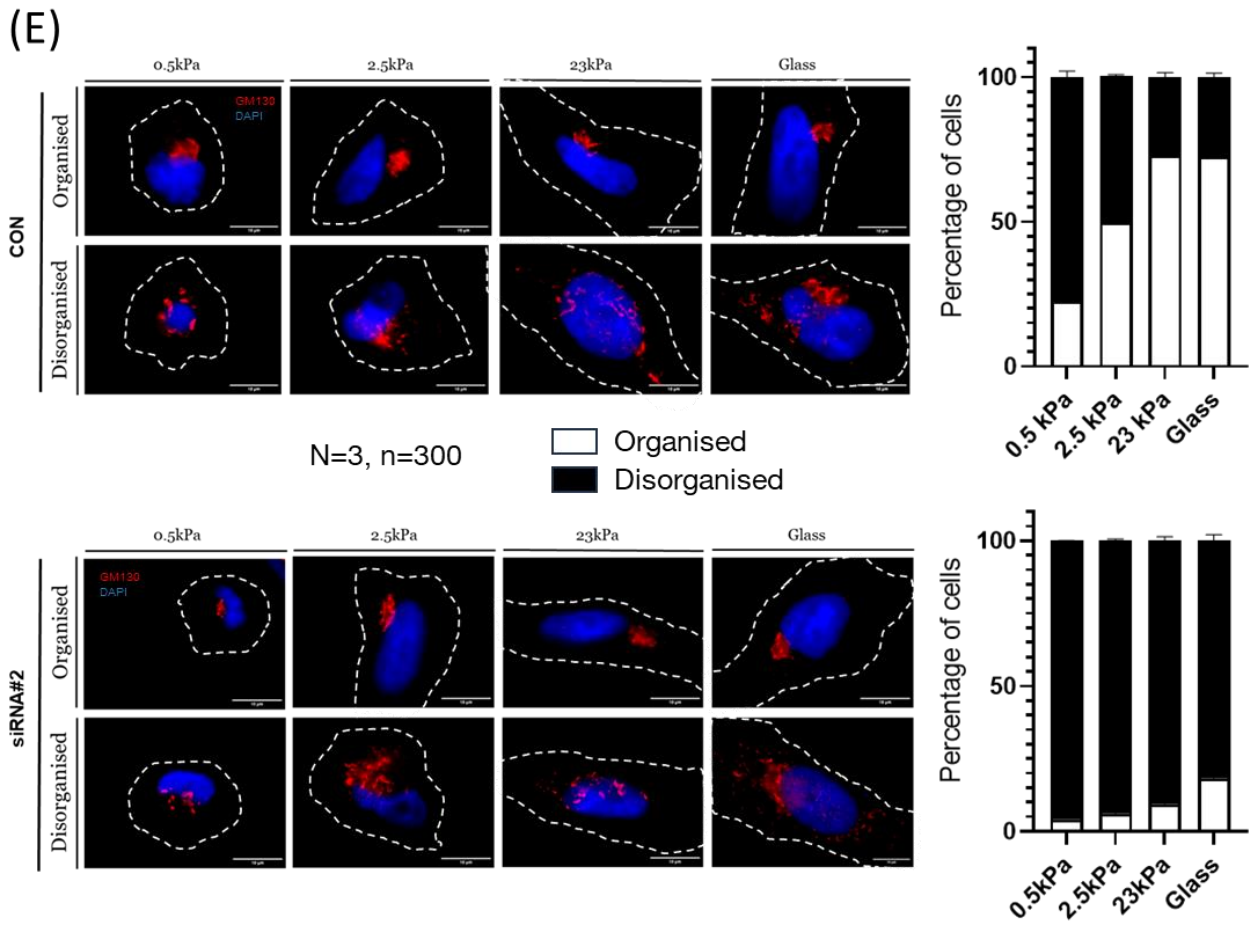
(E)
0.5kPa
2.5kPa
23kPa
Glass
CON
Organised
Disorganised
GM130
DAPI
Percentage of cells
100
50
0
0.5 kPa
2.5 kPa
23 kPa
Glass
N=3, n=300
Organised
Disorganised
siRNA#2
0.5kPa
2.5kPa
23kPa
Glass

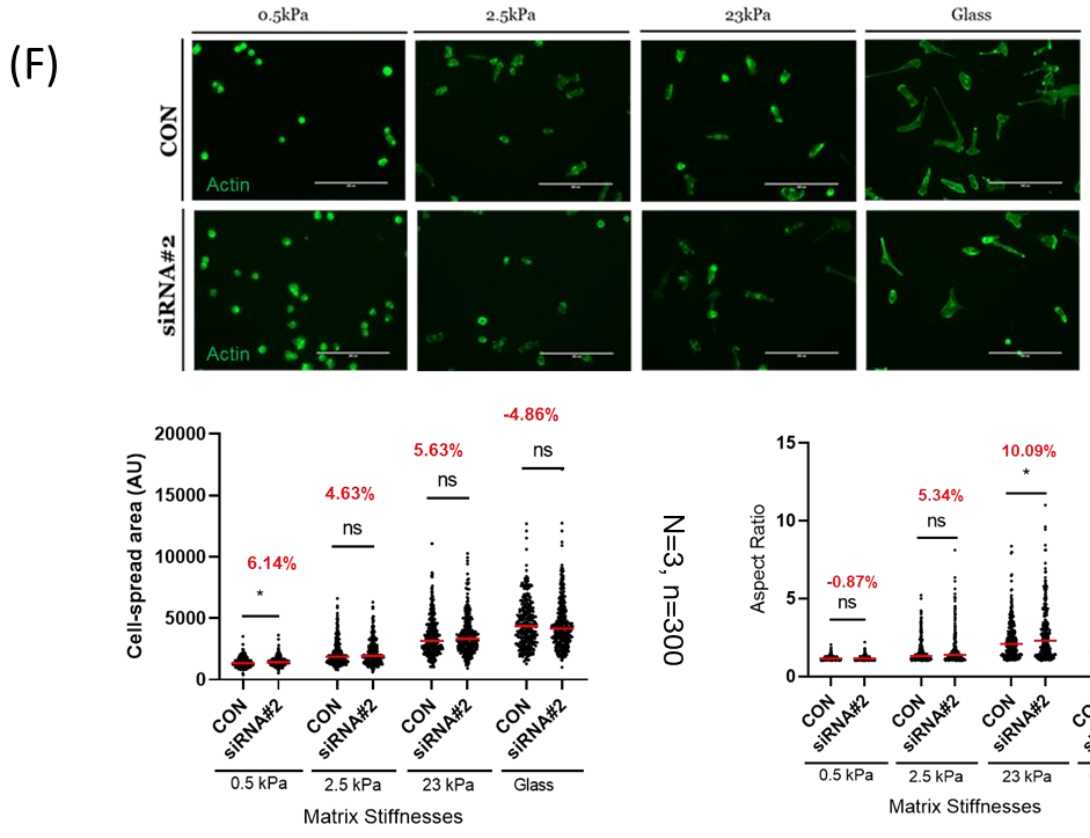
(F)
0.5kPa
2.5kPa
23kPa
Glass
CON
siRNA#2
Actin
Cell-spread area (AU)
20000
15000
10000
5000
0
6.14%
4.63%
5.63%
-4.86%
*
ns
CON
siRNA#2
0.5 kPa
2.5 kPa
23 kPa
Glass
Matrix Stiffnesses
N=3, n=300
Aspect Ratio
15
10
5
0
-0.87%
5.34%
10.09%
13.34%
ns
*
Matrix Stiffnesses

(G)

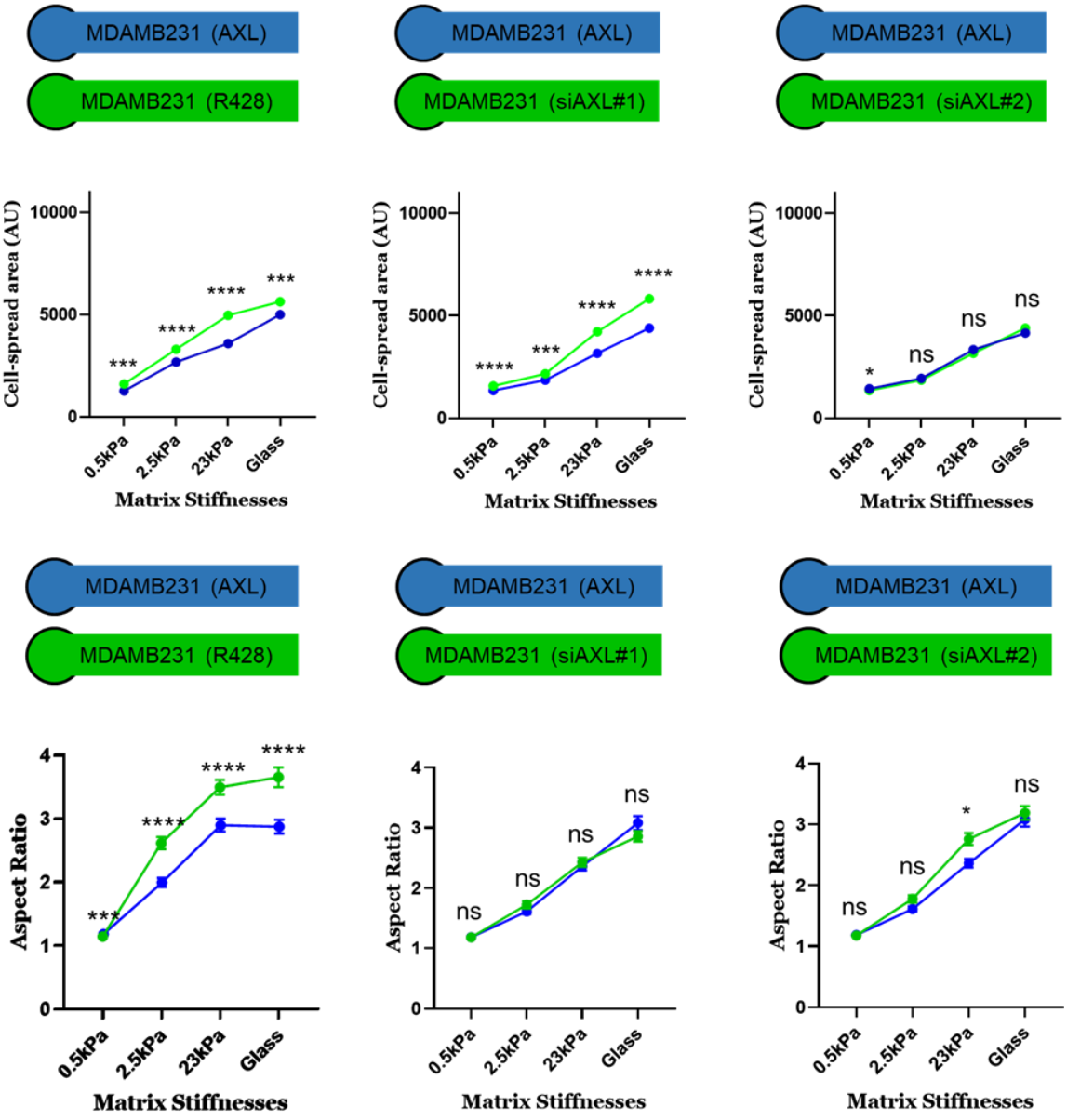
MDAMB231 (AXL)
MDAMB231 (R428)
MDAMB231 (siAXL#1)
MDAMB231 (siAXL#2)
Cell-spread area (AU)
Aspect Ratio
0.5kPa
2.5kPa
23kPa
Glass
Matrix Stiffnesses
ns

(H)

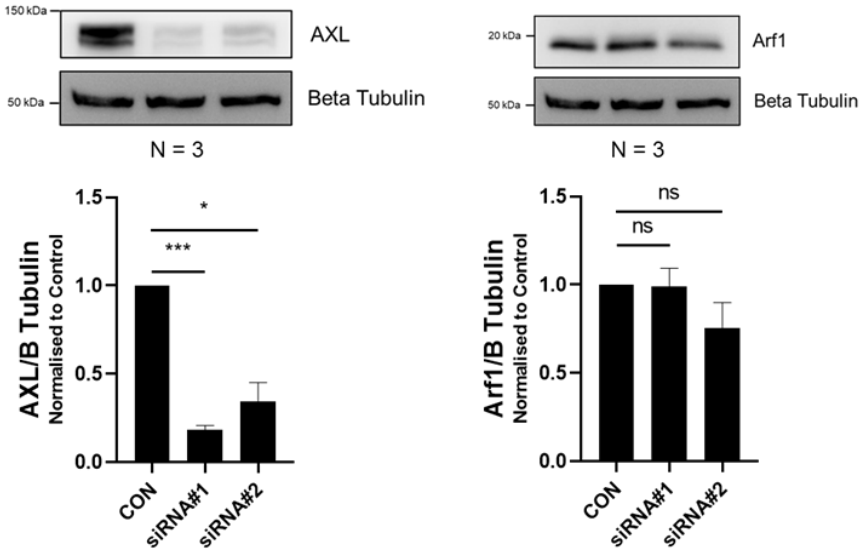
150 kDa
AXL
50 kDa
Beta Tubulin
N = 3
20 kDa
Arf1
AXL/B Tubulin
Normalised to Control
Arf1/B Tubulin
CON
siRNA#1
siRNA#2
ns

Figure 3.2: *MDAMB231 cells were seeded on the 2D hydrogels of the varying matrix stiffnesses and were treated for the R428 for 12 hrs. Then, they were stained for the Golgi (anti-GM130) and actin (phalloidin 488). (A) Images represent the Golgi organization phenotypes at the respective stiffnesses, and the graph next to them shows the Golgi organization distribution profile of MDAMB231 upon R428 treatment. (B) Images represent the spreading of the cells, and two graphs next to them show the cell-spread area and aspect ratio of MDAMB231 cells on 2D hydrogels upon the R428 treatment. (C, E) Images represent the Golgi organization phenotypes at the respective stiffnesses, and the graph next to them shows the Golgi organization distribution profile of MDAMB231 upon AXL KD using siAXL#1 and siAXL#2, respectively. (D, F) Images represent the spreading of the cells, and two graphs next to them, cell-spread area and aspect ratio of MDAMB231 cells on 2D hydrogels upon AXL KD using siAXL#1 and siAXL#2, respectively. (G) Comparison of cell-spread area and aspect ratio between the MDAMB231 upon R428 treatment vs. DMSO. (H) Western blot will show the efficiency of the AXL KD using both siRNAs. The second graph shows AXL KD's effects on the total Arf1 expression levels.*

characterized the mechano-responsiveness of the Golgi secretory trafficking, governed by changing matrix stiffness and the transmission of the mechanical forces via the actomyosin machinery.

AXL being a Golgi regulator and having a known crosstalk with the actomyosin machinery, we wanted to check if AXL has any role in regulating cellular spreading and polarity, which will further suggest a role for AXL in mechanosensory pathways in MDAMB231 cells. R428 mediated AXL inhibition on MDAMB231 cells seeded on the varying matrix stiffnesses, was seen to increase cell-spread area and aspect ratio across all increasing stiffnesses when compared to DMSO-treated control cells. This suggested that AXL inhibition and its possible regulation of cell-adhesion-dependent actin dynamics could affect spread area and polarity. AXL knockdown using both the siRNAs (siAXL#1 and siAXL#2) showed variable effects on cell spreading and aspect ratio. siRNA AXL#1 affected cell spreading across 2D gels of increasing stiffness comparable to R428 inhibition. However, no significant effect on cell aspect ratio was seen, unlike on R428 inhibition. siAXL#2 knockdown interestingly did not significantly affect cell spread are or cell aspect ratio. This despite the fact that both siRNA is able to regulate matrix stiffness dependent Golgi organisation. This raises the need to test the specificity of the inhibitor and also confirming the specificity of the knockdown by reconstitution studies using siRNA-resistant AXL mutants. This also suggests that

AXL-mediated regulation of Golgi organisation may not directly be connected to the stiffness-dependent regulation of cell spreading and polarization. Hence, there arises a possibility of these cell spreading and cell polarization being regulated by AXL via Golgi. Or these could be even AXL-dependent but Golgi independent.

3.3: Role of AXL in Golgi organization and cell spreading in MCF7 cells.

So far, all our evaluations on Golgi organization as a response to cellular mechanosensing have looked at MDAMB231 cells, which have very high AXL expression and activation. To confirm the role of AXL as a mehanosensitive regulator of the Golgi, we extended this hypothesis to MCF7 cells, which inherently have poor AXL protein expression. Reconstituting AXL expression in MCF7 cells to examine its effect on matrix stiffness dependent Golgi organization and cell spreading, could further help establish its role. We first optimised the transient expression of AXL-GFP in MCF7 cells which was seen to drive Golgi organization in MCF7 cells. Quantitative evaluation confirmed a significant reduction in the number of distinct Golgi objects in AXL-GFP expressing MCF7 cells compared to control cells (Figure 3A). Confocal images revealed that the Golgi, rather than being radially distributed around the nucleus, shows a polarised perinuclear organization. This distinct Golgi phenotype with reduced Golgi object counts and polarised perinuclear organization was observed in ~70% of AXL-GFP expressing cells.

To check Golgi organization on the matrices of varying stiffnesses, we need an MCF7 cell line where AXL is stably expressed. We hence went on the generate a stable AXL expressing MCF7 cell line using a retroviral AXL-pBABE puro plasmid vector. The protocol used in generating the stable AXL-MCF7 cells involved the conventional retroviral transduction steps where HEK293T cells were transfected with retroviral packaging plasmids along with the AXL-pBABE puro plasmid to generate viral particles, which were subsequently used for transduction MCF7 cells followed by puromycin selection (Figure 3B).

(A)

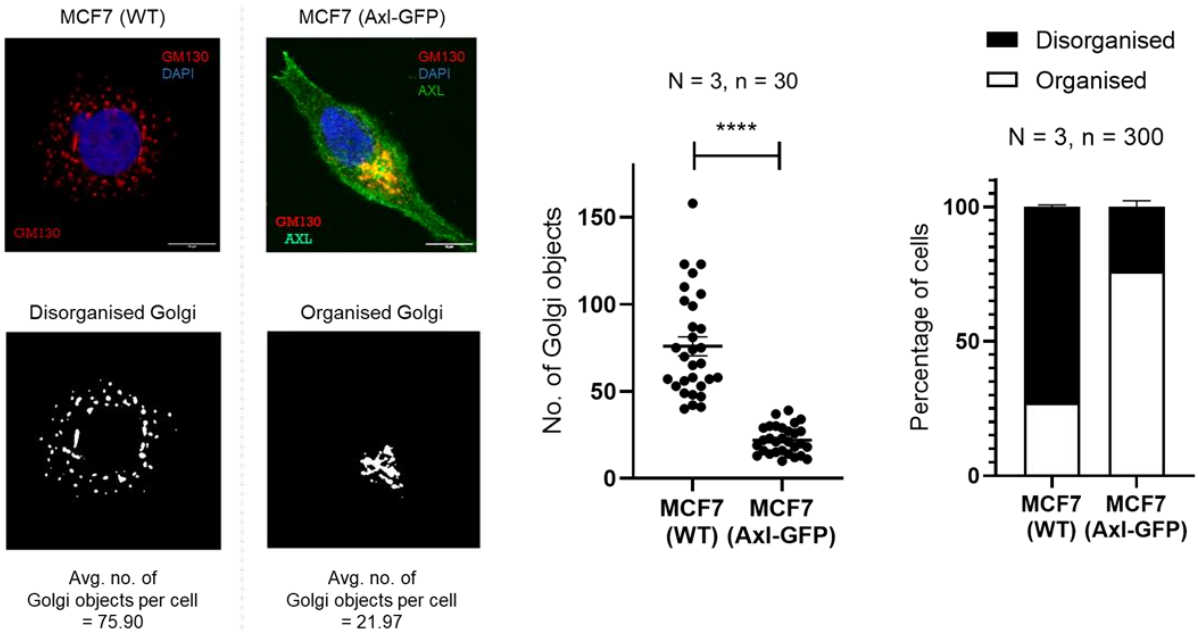
MCF7 (WT)
GM130
DAPI
GM130
MCF7 (Axl-GFP)
GM130
DAPI
AXL
GM130
AXL
Disorganised Golgi
Organised Golgi
Avg. no. of
Golgi objects per cell
= 75.90
Avg. no. of
Golgi objects per cell
= 21.97
N = 3, n = 30
****
No. of Golgi objects
150
100
50
0
MCF7
(WT)
MCF7
(Axl-GFP)
Disorganised
Organised
N = 3, n = 300
Percentage of cells
100
50
0
MCF7
(WT)
MCF7
(Axl-GFP)

(B)


1
HEK293T cell seeding
3*6 cm dishes
1.5 Lakh cells in each dish
24 hrs
2
Transfection with plasmids
Each dish transfected with plasmids
As shown in schematic below.
48 hrs
3
Add 2 ml 10% DMEM
Extra 2 ml 10% DMEM
Seed 3*35 mm dishes 1.5 Lakh MCF7
24 hrs
4
Viral Titter addition to the MCF7
Viral Titter (3 ml) + 10%DMEM (1 ml)
+ Polybrene (4 µl of 10 mg/ml).
MCF7 confluency~ 50%
72 hrs
5
Start puromycin selection
Puromycin working conc. = 1.6 µg/ml
72 hrs
6
Checking cell viability
Check the cell viability for next 72 hrs
(if needed for 96 hrs)
7
Replating cells & wait to grow
After getting the transduced colonies, split them into the 24 well-plate
HEK239T
Plasmids:
pVSVG - 2 µg
pGagPol - 3 µg
EmptypBABE puro - 4 µg
HEK239T
Plasmids:
pVSVG - 2 µg
pGagPol - 3 µg
AxlpBABE puro- 4 µg
HEK239T
Plasmids:
pVSVG - 2 µg
pGagPol - 3 µg
pMIG – 7.5 µg

(C)

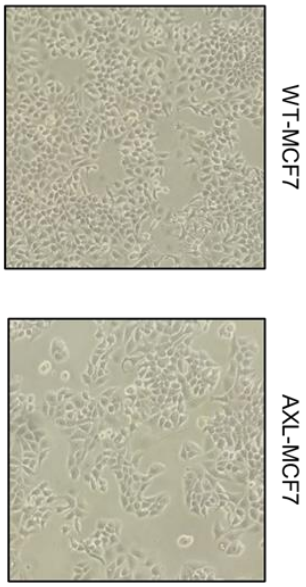
WT-MCF7
AXL-MCF7

(D)

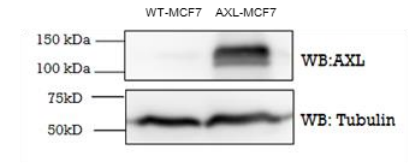
WT-MCF7
AXL-MCF7
150 kDa
100 kDa
WB:AXL
75kD
50kD
WB: Tubulin

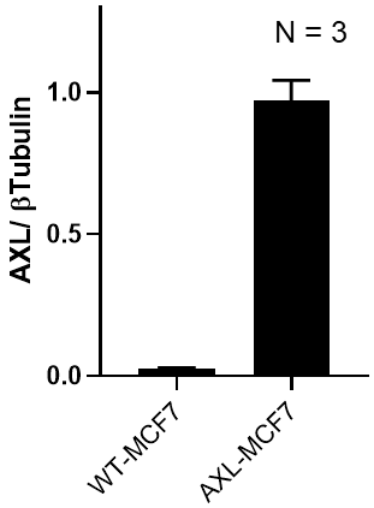
N = 3
AXL/ βTubulin
1.0
0.5
0.0
WT-MCF7
AXL-MCF7

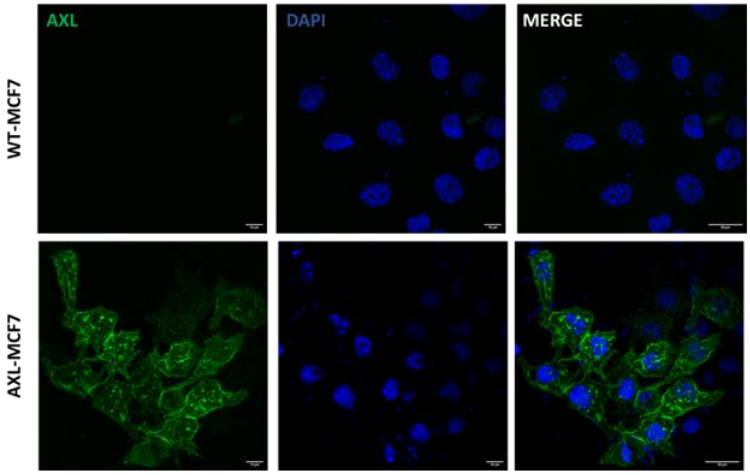
AXL
DAPI
MERGE
WT-MCF7
AXL-MCF7

(E)

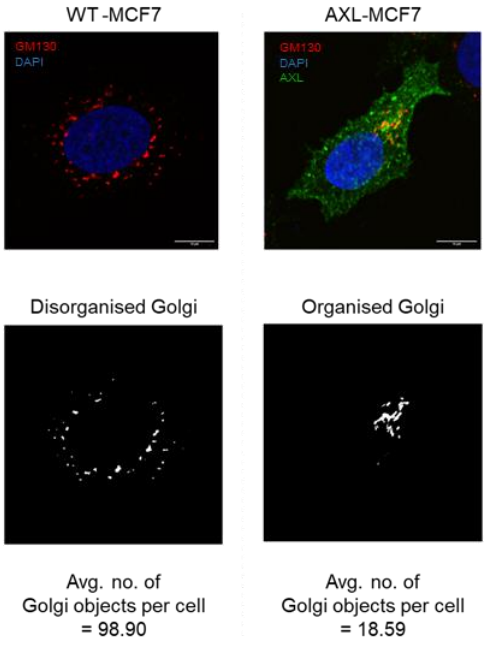
WT-MCF7
AXL-MCF7
GM130
DAPI
AXL
Disorganised Golgi
Organised Golgi
Avg. no. of Golgi objects per cell = 98.90
Avg. no. of Golgi objects per cell = 18.59

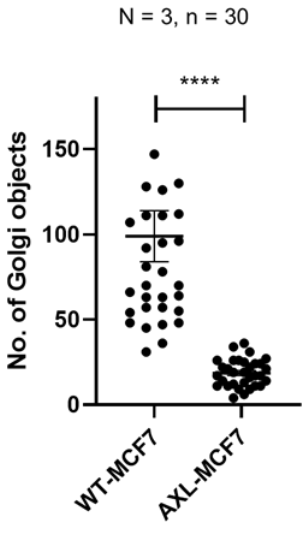
N = 3, n = 30
****
No. of Golgi objects
150
100
50
0
WT-MCF7
AXL-MCF7

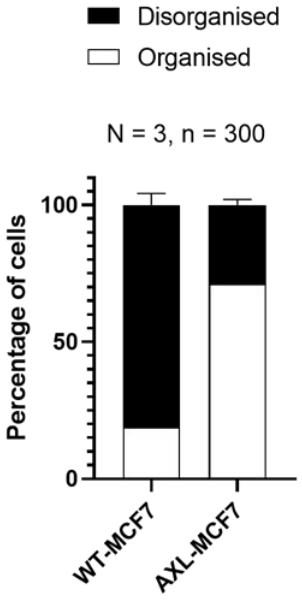
Disorganised
Organised
N = 3, n = 300
Percentage of cells
100
50
0
WT-MCF7
AXL-MCF7

Figure 3.3: *(A) Images represent the effect transient AXL expression has on the Golgi organization. Graphs show the number of the Golgi particles in the MCF7 cells vs. MCF7 cells expressing the AXL-GFP construct, and also, the Golgi organization distribution profile represents the percentage of cells showing organized vs. disorganized Golgi. (B) The schematic shows the protocol followed to make the AXL-MCF7 cell line. (C) Representative bright field images for the WT-MCF7 and AXL-MCF7 cell lines. (D) The stable integration of the AXL in the MCF7 cells was confirmed using western blotting, and lysates were prepared from the three independent experiments. (E) Images represent the Golgi organization in the WT-MCF7 and AXLMCF7 cells. Graphs show the number of the Golgi particles in the WT-MCF7 cells vs. AXL-MCF7, and also, the Golgi organization distribution profile represents the percentage of cells showing organized vs. disorganized Golgi phenotype.*

To confirm the expression of the AXL in the selected colonies, we did western blotting to check AXL protein levels as compared to wild-type MCF7 cells. This was followed by immunostaining with anti-AXL antibody to confirm expression and localization of AXL in the selected cell population (Figure 3C). AXL expression and localization were also confirmed by staining both these cells with anti-AXL antibodies, as you can see in Figure 3C, which shows the presence and localization of the AXL in the AXL-MCF7 cells. However, no staining is observed in WT-MCF7 cells.

Once the stable reconstitution of AXL was confirmed in MCF7 cells, we wanted to check whether AXL expression could similarly affect the Golgi organization of MCF7 cells, as observed on transient AXL expression. Similar results were observed when a quantitative evaluation of Golgi object count was performed for WT and Stable AXL-MCF7 cells. There was a significant reduction in the number of Golgi objects for cells showing AXL expression. Also, a similar polarised perinuclear Golgi phenotype was observed as seen with transient AXL expression in MCF7 cells. The Golgi distribution profile revealed stable AXL-MCF7 cells showed a distinctly higher percentage of cells with organized Golgi than WT cells. These observations further confirm our initial hypothesis that AXL expression acts as a regulator of Golgi organization in MDAMB231 and MCF7 cells.

Immediate plans aim to test if stable expression of AXL (stable AXL-MCF7) restores matrix stiffness dependent regulation of Golgi organisation, comparable to MDAMB231 cells. It will also be worth checking how the impact AXL has on Golgi-dependent functional processes, like trafficking and cell-surface glycosylation could

affect cell function in MDAMB231 vs MCF7 vs AXL-MCF7 cells. The impact this has on malignant transformation of cells affecting cell migration, invasion, and anchorage-independent growth.

3.4: Protein expression levels on varying matrix stiffnesses for MDAMB231 cells.

Earlier studies suggest differential expression of genes in cells on matrices of varying stiffnesses (Zhang et al., 2022) could affect their role. As a first step towards understanding whether AXL expression and activation are mechanosensitive, we tested total AXL expression in MDAMB231 on increasing matrix stiffness. Quantitative western blot shows total AXL protein levels to significantly increase with increasing matrix stiffness. This could reflect a transcriptional or post-transcriptional mechanism by which matrix stiffness could alter the AXL protein levels. The activation status of AXL (phospho-AXL) across these stiffnesses remains to be tested.

Previously, we discussed the role Arf1 has in the adhesion-dependent regulation of Golgi organization in MDAMB231, which is likely mediated via the AXL-Arf1 crosstalk. Total Arf1 expression levels on the varying matrix stiffnesses, showed a significant increase. This could reflect the possible regulation of AXL and Arf1 could be mediated along comparable pathways. Upon R428 treatment, active Arf1 levels were shown to drop, contributing to Golgi's disorganisation in MDAMB231 (Fig 1.8B). Also, upon loss of adhesion in MDAMB31, active Arf1 levels drop, which could be the driving factor for Golgi disorganization upon suspension (Unpublished data from the lab). Hence, lower Arf1 expression (or activation) on lower stiffnesses could contribute to the disorganized Golgi phenotype on lower stiffness.

The rapid acetylation of the microtubules (MTs) derived from the Golgi, which are newly nucleated (Chabin-Brion et al.), and the depletion of most of the MT stabilizers, disturbs the Golgi complex integrity, which is a well-known function of the Golgi derived MTs. As a readout of the effect of changing Golgi organization on changing matrix stiffness in MDAMB231, we could look at microtubule acetylation levels. This reflects Golgi-associated microtubules which are affected by Golgi organisation. There is also

literature suggesting that matrix stiffness can affect the acetylation of the microtubules. One of the studies done in a pathological condition named skin fibrosis has shown that α-tubulin acetylation is required for fibroblast activation, and it is shown to be associated with the biomechanics-induced upregulation of the K40 acetylation, which in turn promotes fibrosis by cytoplasm-nucleus shuttle of Yes-associated protein. α-tubulin N-acetyltransferase 1 (α-TAT1) mediated acetylation of the microtubules, which is a post-translational modification, promotes microtubule stability in response to mechanical stimulation (Wen et al.). The study by Li et al. has also shown that silica, matrix stiffening, and even combination can lead to the downregulation of the acetylated α-Tubulin in alveolar epithelial cells. We hence evaluated the acetylation status of microtubules across varying matrix stiffness by quantitative western blotting. This showed increasing microtubule acetylation levels with increasing matrix stiffness when normalized to total tubulin levels. This correlates with the Golgi being predominantly organized at higher stiffness.

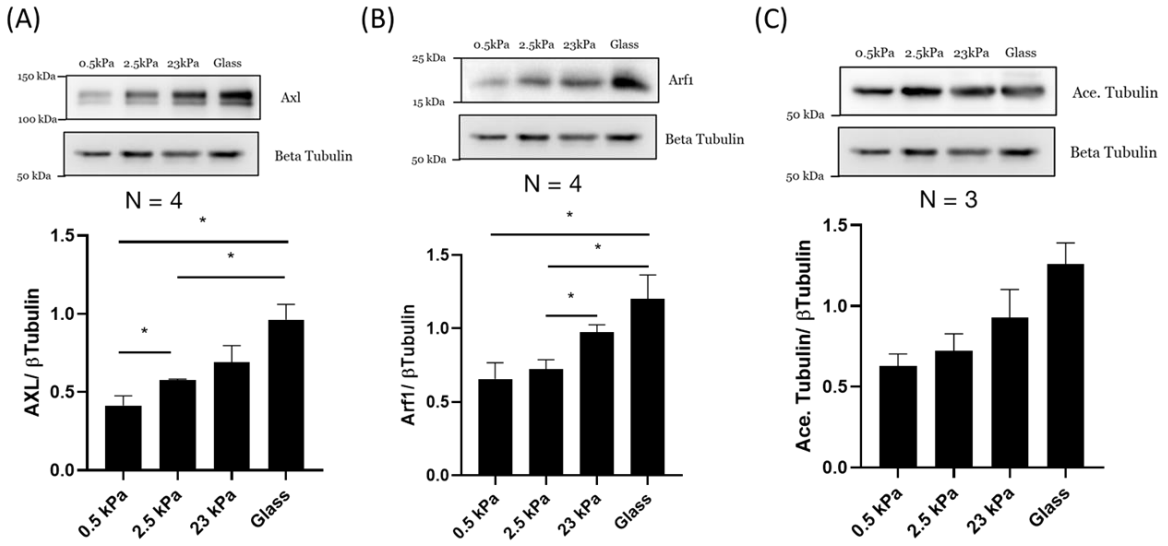

Figure 3.4: *MDAMB231 cells were seeded on the 2D hydrogels for 24 hrs and were lysed. These lysates were probed for the different proteins as follows. (A) Cell lysates were probed for AXL. The graph below the representative blots shows the band intensity ratio of AXL to Beta Tubulin from four independent experiments with their SEM. (B) Cell lysates were probed for Arf1. The graph above the representative blots shows the band intensity ratio of Arf1 to beta-tubulin from 4 independent experiments with their SEM. (C) Cell lysates were probed for acetylated tubulin. The graph below the representative blots shows the band intensity ratio of acetylated tubulin to Beta Tubulin from three independent experiments with their SEM.*

Given that we have looked at the levels of AXL and Arf1 on the varying matrix stiffnesses, it is worth asking what lower expression levels of AXL and Arf1 mean on the soft matrices. Also, is the disorganization of the Golgi on lower stiffnesses happening through the AXL-Arf1 mechanism, as we saw in the case of R428-mediated Golgi disorganization in MDAMB231? Hence, looking at the active Arf1 levels on the varying matrix stiffnesses could reveal more about this regulation. This can be addressed using a GGA3 pull-down of active Arf1 in cell lysates from varying matrix stiffnesses.

Our data suggests that AXL-Arf1 crosstalk could regulate the adhesion-dependent Golgi organization in the breast cancer cells (MDAMB231 vs MCF7 cells). The role AXL-Arf1 crosstalk could have in the stiffness-dependent regulation of Golgi organization is worth evaluating going forward. The impact stiffness-dependent Golgi organisation could have in regulating Golgi function is also worth evaluating. Understanding if and how this regulation works in normal cells in response to changing matrix stiffness is also worth testing.

References:

Ahat, E., Y. Xiang, X. Zhang, M.E. Bekier Ll, and Y. Wang. 2019. GRASP depletion-mediated Golgi destruction decreases cell adhesion and migration via the reduction of α5β1 integrin. *Mol Biol Cell*. 30. doi:10.1091/mbc.E18-07-0462.

Barzilai, S., S.K. Yadav, S. Morrell, F. Roncato, E. Klein, L. Stoler-Barak, O. Golani, S.W. Feigelson, A. Zemel, S. Nourshargh, and R. Alon. 2017. Leukocytes Breach Endothelial Barriers by Insertion of Nuclear Lobes and Disassembly of Endothelial Actin Filaments. *Cell Rep*. 18. doi:10.1016/j.celrep.2016.12.076.

Carsten Johannes Helle, S., Q. Feng, M.J. Aebersold, L. Hirt, R.R. Grü ter, A. Vahid, A. Sirianni, S. Mostowy, J.G. Snedeker, A.S. ˇ aric, T. Idema, T. Zambelli, and B. Kornmann. 2017. Mechanical force induces mitochondrial fission. doi:10.7554/eLife.30292.001.

Dahl, K.N., S.M. Kahn, K.L. Wilson, and D.E. Discher. 2004. The nuclear envelope lamina network has elasticity and a compressibility limit suggestive of a molecular shock absorber. *J Cell Sci*. 117. doi:10.1242/jcs.01357.

Donaldson, J.G., A. Honda, and R. Weigert. 2005. Multiple activities for Arf1 at the Golgi complex. *Biochim Biophys Acta Mol Cell Res*. 1744. doi:10.1016/j.bbamcr.2005.03.001.

Elgindi, M., J. Sapudom, I.H. Ibrahim, M. Al-Sayegh, W. Chen, A. Garcia-Sabaté, and J.C.M. Teo. 2021. May the force be with you (Or not): The immune system under microgravity. *Cells*. 10. doi:10.3390/cells10081941.

Feng, Q., and B. Kornmann. 2018. Mechanical forces on cellular organelles. *J Cell Sci*. 131. doi:10.1242/jcs.218479.

Guadamillas, M.C., A. Cerezo, and M.A. del Pozo. 2011. Overcoming anoikis - pathways to anchorageindependent growth in cancer. *J Cell Sci*. 124. doi:10.1242/jcs.072165.

Guet, D., K. Mandal, M. Pinot, J. Hoffmann, Y. Abidine, W. Sigaut, S. Bardin, K. Schauer, B. Goud, and J.B. Manneville. 2014. Mechanical role of actin dynamics in the rheology of the Golgi complex and in Golgi-associated trafficking events. *Current Biology*. 24. doi:10.1016/j.cub.2014.06.048.

Van Helvert, S., C. Storm, and P. Friedl. 2018. Mechanoreciprocity in cell migration. *Nat Cell Biol*. 20. doi:10.1038/s41556-017-0012-0.

Huang, S., and D.E. Ingber. 1999. The structural and mechanical complexity of cell-growth control. *Nat Cell Biol*. 1. doi:10.1038/13043.

Iskratsch, T., H. Wolfenson, and M.P. Sheetz. 2014. Appreciating force and shape-the rise of mechanotransduction in cell biology. *Nat Rev Mol Cell Biol*. 15. doi:10.1038/nrm3903.

Jaalouk, D.E., and J. Lammerding. 2009. Mechanotransduction gone awry. *Nat Rev Mol Cell Biol*. 10. doi:10.1038/nrm2597.

Jansen, K.A., P. Atherton, and C. Ballestrem. 2017. Mechanotransduction at the cell-matrix interface. *Semin Cell Dev Biol*. 71. doi:10.1016/j.semcdb.2017.07.027.

Kechagia, J.Z., J. Ivaska, and P. Roca-Cusachs. 2019. Integrins as biomechanical sensors of the microenvironment. *Nat Rev Mol Cell Biol*. 20. doi:10.1038/s41580-019-0134-2.

Khalili, A.A., and M.R. Ahmad. 2015. A Review of cell adhesion studies for biomedical and biological applications. *Int J Mol Sci*. 16. doi:10.3390/ijms160818149.

Kraus, F., K. Roy, T.J. Pucadyil, and M.T. Ryan. 2021. Function and regulation of the divisome for mitochondrial fission. *Nature*. 590. doi:10.1038/s41586-021-03214-x.

Liu, C., M. Li, Z.X. Dong, D. Jiang, X. Li, S. Lin, D. Chen, X. Zou, X.D. Zhang, and G.D. Luker. 2021. Heterogeneous microenvironmental stiffness regulates pro-metastatic functions of breast cancer cells. *Acta Biomater*. 131. doi:10.1016/j.actbio.2021.07.009.

Liu, Z., J.L. Tan, D.M. Cohen, M.T. Yang, N.J. Sniadecki, S.A. Ruiz, C.M. Nelson, and C.S. Chen. 2010. Mechanical tugging force regulates the size of cell-cell junctions. *Proc Natl Acad Sci U S A*. 107. doi:10.1073/pnas.0914547107.

Moore, A.S., Y.C. Wong, C.L. Simpson, and E.L.F. Holzbaur. 2016. Dynamic actin cycling through mitochondrial subpopulations locally regulates the fission-fusion balance within mitochondrial networks. *Nat Commun*. 7. doi:10.1038/ncomms12886.

Panciera, T., L. Azzolin, M. Cordenonsi, and S. Piccolo. 2017. Mechanobiology of YAP and TAZ in physiology and disease. *Nat Rev Mol Cell Biol*. 18. doi:10.1038/nrm.2017.87.

Paszek, M.J., and V.M. Weaver. 2004. The tension mounts: Mechanics meets morphogenesis and malignancy. *J Mammary Gland Biol Neoplasia*. 9. doi:10.1007/s10911-004-1404-x.

Paul, M.K., and A.K. Mukhopadhyay. 2012. Tyrosine kinase – Role and significance in Cancer. *Int J Med Sci*. doi:10.7150/ijms.1.101.

Petrosyan, A. 2015. Onco-Golgi: Is Fragmentation a Gate to Cancer Progression? *Biochem Mol Biol J*. 01. doi:10.21767/2471-8084.100006.

Phuyal, S., P. Romani, S. Dupont, and H. Farhan. 2023. Mechanobiology of organelles: illuminating their roles in mechanosensing and mechanotransduction. *Trends Cell Biol*. 33. doi:10.1016/j.tcb.2023.05.001.

Plotnikov, S. V., A.M. Pasapera, B. Sabass, and C.M. Waterman. 2012. Force fluctuations within focal adhesions mediate ECM-rigidity sensing to guide directed cell migration. *Cell*. 151. doi:10.1016/j.cell.2012.11.034.

Ravichandran, Y., B. Goud, and J.B. Manneville. 2020. The Golgi apparatus and cell polarity: Roles of the cytoskeleton, the Golgi matrix, and Golgi membranes. *Curr Opin Cell Biol*. 62. doi:10.1016/j.ceb.2019.10.003.

Romani, P., I. Brian, G. Santinon, A. Pocaterra, M. Audano, S. Pedretti, S. Mathieu, M. Forcato, S. Bicciato, J.B. Manneville, N. Mitro, and S. Dupont. 2019. Extracellular matrix mechanical cues regulate lipid metabolism through Lipin-1 and SREBP. *Nat Cell Biol*. 21. doi:10.1038/s41556-018-0270-5.

Singh, V., C. Erady, and N. Balasubramanian. 2018. Cell-matrix adhesion controls Golgi organization and function through Arf1 activation in anchorage-dependent cells. *J Cell Sci*. 131. doi:10.1242/jcs.215855.

Sun, Z., S.S. Guo, and R. Fässler. 2016. Integrin-mediated mechanotransduction. *Journal of Cell Biology*. 215. doi:10.1083/jcb.201609037.

Tan, X., L. Shi, P. Banerjee, X. Liu, H.F. Guo, J. Yu, N. Bota-Rabassedas, B.L. Rodriguez, D.L. Gibbons, W.K. Russell, C.J. Creighton, and J.M. Kurie. 2021. A

protumorigenic secretory pathway activated by p53 deficiency in lung adenocarcinoma. *Journal of Clinical Investigation*. 131. doi:10.1172/JCI137186.

Urra, F.A., S. Fuentes-Retamal, C. Palominos, Y.A. Rodríguez-Lucart, C. López-Torres, and R. Araya-Maturana. 2021. Extracellular Matrix Signals as Drivers of Mitochondrial Bioenergetics and Metabolic Plasticity of Cancer Cells During Metastasis. *Front Cell Dev Biol*. 9. doi:10.3389/fcell.2021.751301.

Xiang, Y., X. Zhang, D.B. Nix, T. Katoh, K. Aoki, M. Tiemeyer, and Y. Wang. 2013. Regulation of protein glycosylation and sorting by the Golgi matrix proteins GRASP55/65. *Nat Commun*. 4. doi:10.1038/ncomms2669.

Xu, R., P. Yin, J. Wei, and Q. Ding. 2023. The role of matrix stiffness in breast cancer progression: a review. *Front Oncol*. 13. doi:10.3389/fonc.2023.1284926.

Yang, B., Z.Z. Lieu, H. Wolfenson, F.M. Hameed, A.D. Bershadsky, and M.P. Sheetz. 2016. Mechanosensing Controlled Directly by Tyrosine Kinases. *Nano Lett*. 16. doi:10.1021/acs.nanolett.6b02995.

Yue, B. 2014. Biology of the extracellular matrix: An overview. *J Glaucoma*. 23:S20–S23. doi:10.1097/IJG.0000000000000108.

Zdzalik-Bielecka, D., A. Poswiata, K. Kozik, K. Jastrzebski, K.O. Schink, M. Brewinska-Olchowik, K. Piwocka, H. Stenmark, and M. Miaczynska. 2021. The GAS6-AXL signaling pathway triggers actin remodeling that drives membrane ruffling, macropinocytosis, and cancer-cell invasion. *Proc Natl Acad Sci U S A*. 118. doi:10.1073/pnas.2024596118.

Zhang, C., X. Han, J. Xu, and Y. Zhou. 2022. Matrix Stiffness-Induced Transcriptome Alterations and Regulatory Mechanisms Revealed by RNA-Seq in Endothelial Cells. *J Biomater Nanobiotechnol*. 13. doi:10.4236/jbnb.2022.133004.

Wen, Dongsheng, et al. “Matrix Stiffness-Induced α-Tubulin Acetylation Is Required for Skin Fibrosis Formation through Activation of Yes-Associated Protein.” *MedComm*, vol. 4, no. 4, 12 July 2023, https://doi.org/10.1002/mco2.319. Accessed 20 Mar. 2024.

Li, Gengxu, et al. “Matrix Stiffness Regulates α-TAT1-Mediated Acetylation of α-Tubulin and Promotes Silica-Induced Epithelial–Mesenchymal Transition via DNA

Damage.” *Journal of Cell Science*, vol. 134, no. 2, 15 Jan. 2021, journals.biologists.com/jcs/article/134/2/jcs243394/224091/Matrix-stiffness-regulates-TAT1-mediated, https://doi.org/10.1242/jcs.243394. Accessed 20 Mar. 2024.

Liu, Chun, et al. “Heterogeneous Microenvironmental Stiffness Regulates Pro-Metastatic Functions of Breast Cancer Cells.” *Acta Biomaterialia*, vol. 131, Sept. 2021, pp. 326–340, https://doi.org/10.1016/j.actbio.2021.07.009. Accessed 19 Mar. 2023.

Chabin-Brion, Karine, et al. “The Golgi Complex Is a Microtubule-Organizing Organelle.” *Molecular Biology of the Cell*, vol. 12, no. 7, July 2001, pp. 2047–2060, https://doi.org/10.1091/mbc.12.7.2047. Accessed 25 July 2022.

Theodossiou, Theodossis A., et al. “Simultaneous Defeat of MCF7 and MDA-MB-231 Resistances by a Hypericin PDT–Tamoxifen Hybrid Therapy.” *Npj Breast Cancer*, vol. 5, no. 1, 10 Apr. 2019, https://doi.org/10.1038/s41523-019-0108-8.

Copeland, Sarah J., et al. “Actin- and Microtubule-Dependent Regulation of Golgi Morphology by FHDC1.” *Molecular Biology of the Cell*, vol. 27, no. 2, 15 Jan. 2016, pp. 260–276, https://doi.org/10.1091/mbc.e15-02-0070. Accessed 30 Aug. 2022.